Set Oriented Numerical Methods for Dynamical Systems

Michael Dellnitz and Oliver Junge

Department of Mathematics and Computer Science
University of Paderborn
D-33095 Paderborn

http://www.upb.de/math/~agdellnitz

November 5, 2004

Contents

1 Introduction **1**

2 The Computation of Invariant Sets **2**
2.1 Brief Review on Invariant Sets 2
2.2 The Computation of Relative Global Attractors 3
2.3 Convergence Behavior and Error Estimate 5
2.4 Numerical Examples 8
2.5 The Computation of Chain Recurrent Sets 9
2.6 Numerical Example 11

3 The Computation of Invariant Manifolds **12**
3.1 Description of the Method 13
3.2 Convergence Behavior and Error Estimate 14
3.3 Numerical Examples 15

4 The Computation of SRB-Measures **18**
4.1 Brief Review on SRB-Measures and Small Random Perturbations 20
4.2 Spectral Approximation for the Perron-Frobenius Operator . . 23
4.3 Convergence Result for SRB-Measures 26
4.4 Numerical Examples 26

5 The Identification of Cyclic Behavior **28**
5.1 Extraction of Cyclic Behavior 28
5.2 Numerical Examples 30

6 The Computation of Almost Invariant Sets **32**
6.1 Almost Invariant Sets 33
6.2 Numerical Examples 36

7 Adaptive Subdivision Strategies **37**
7.1 Adaptive Subdivision Algorithm 38
7.2 Numerical Examples 40

8 Implementational Details **41**
8.1 Realization of the Collections and the Subdivision Step 42
8.2 Realization of the Intersection Test 43
8.3 Implementation of the Measure Computation 47

References **48**

1 Introduction

Over the past years so-called *set oriented* numerical methods have been developed for the study of complicated temporal behavior of dynamical systems. These numerical tools can be used to approximate different types of invariant sets or invariant manifolds but they also allow to extract statistical information on the dynamical behavior via the computation of natural invariant measures or almost invariant sets. In contrast to other numerical techniques these methods do not rely on the computation of *single* long term trajectories but rather use the information obtained from *several* short term trajectories.

All the methods which are described in this chapter are based on multilevel subdivision procedures for the computation of certain invariant sets. This multilevel approach allows to cover the object of interest – e.g. an invariant manifold or the support of an invariant measure – by several small subsets of state space. Since outer approximations are produced and long term simulations are avoided these methods are typically quite robust. Recently also adaptive subdivision strategies have been developed and moreover concrete realizations have been proposed which allow to make the computations rigorous.

The numerical methods presented here are similar in spirit to the so-called *cell mapping approach*, see e.g. Kreuzer (1987); Hsu (1992). However, a significant difference lies in the fact that in the cell mapping case the numerical effort depends crucially on the dimension of state space whereas for the multilevel subdivision procedures the efficiency essentially depends on the complexity of the underlying dynamics.

We would also like to mention that by now there exist several relevant extensions and adaptations of the set oriented approach as described here. For instance, in Schütte (1999); Deuflhard et al. (2000) the authors develop and analyze set oriented algorithms which can be used for the identification of so-called *conformations* for molecules. Roughly speaking, these are almost invariant sets for a specific type of Hamiltonian systems. Another direction has been considered in Keller and Ochs (1999). There the set oriented approach has been succesfully adapted to the context of random dynamical systems.

In this chapter we give an overview about the developments in the area of set oriented methods for general deterministic dynamical systems. We

report on both theoretical properties of the numerical methods and details concerning the implementation.

2 The Computation of Invariant Sets

In this section we present set oriented multilevel algorithms for the approximation of two different types of invariant sets, namely attracting sets and chain recurrent sets. We demonstrate the usefulness of this multilevel approach by several numerical examples.

2.1 Brief Review on Invariant Sets

We consider discrete dynamical systems

$$x_{j+1} = f(x_j), \quad j = 0, 1, 2, \ldots, \tag{2.1}$$

where $f : \mathbb{R}^n \to \mathbb{R}^n$ is a diffeomorphism and begin by recalling some types of invariant sets of such dynamical systems.

Attracting Sets

A subset $A \subset \mathbb{R}^n$ is called *invariant* if

$$f(A) = A.$$

Moreover, an invariant set A is an *attracting set* with *fundamental neighborhood* U if for every open set $V \supset A$ there is an $N \in \mathbb{N}$ such that $f^j(U) \subset V$ for all $j \geq N$. Observe that if A is invariant then the closure of A is invariant as well. Hence we restrict our attention to closed invariant sets A, and in this case we obtain

$$A = \bigcap_{j \in \mathbb{N}} f^j(U).$$

By definition all the points in the fundamental neighborhood U are attracted by A. For this reason the open set $\cup_{j \in \mathbb{N}} f^{-j}(U)$ is called the *basin of attraction* of A. If the basin of attraction of A is the entire $\mathbb{R}^n$ then A is called the *global attractor*.

REMARKS 2.1 (a) Although the global attractor may not be compact, it typically happens in applications that all the orbits of the underlying

dynamical system eventually lie inside a bounded domain, and in that case the compactness of A immediately follows.

(b) The global attractor contains all the invariant sets of the dynamical system. This can easily be verified using the definitions.

Chain Recurrent Sets

Sometimes it is of interest to analyze the fine-structure of the dynamics on the global attractor. This is e.g. accomplished by extracting *recurrent* subsets. A notion of recurrence which proved to be particularly useful is that of *chain recurrence* (see Conley (1978)):

DEFINITION 2.2 A point $x \in U \subset \mathbb{R}^n$ belongs to the *chain recurrent set* of f in U if for every $\epsilon > 0$ there is an *ϵ-pseudoperiodic orbit* in U containing x, that is, there exists $\{x = x_0, x_1, \ldots, x_{\ell-1}\} \subset U$ such that

$$\|f(x_i) - x_{i+1 \bmod \ell}\| \leq \epsilon \text{ for } i = 0, \ldots, \ell - 1.$$

It is easy to see that the chain recurrent set is closed and invariant.

2.2 The Computation of Relative Global Attractors

We now present an algorithm for the computation of parts of the global attractor of a dynamical system.

Relative Global Attractors

DEFINITION 2.3 Let $Q \subset \mathbb{R}^n$ be a compact set. We define the *global attractor relative to Q* by

$$A_Q = \bigcap_{j \geq 0} f^j(Q). \tag{2.2}$$

In the following remark we summarize some basic properties of A_Q.

REMARKS 2.4 (a) The definition of A_Q in (2.2) implies that $A_Q \subset Q$ and that $f^{-1}(A_Q) \subset A_Q$, but not necessarily that $f(A_Q) \subset A_Q$.

(b) A_Q is compact since Q is compact.

(c) A_Q is a subset of the global attractor A. In fact,

$$A_Q = \{x \in A \ : \ f^{-j}(x) \in Q \text{ for all } j \geq 0\}.$$

(d) Denote by A the global attractor of f. Then in general

$$A_Q \neq A \cap Q.$$

Subdivision Algorithm

The following algorithm provides a method for the approximation of relative global attractors. It generates a sequence $\mathcal{B}_0, \mathcal{B}_1, \ldots$ of finite collections of compact subsets of $\mathbb{R}^n$ such that the diameter

$$\operatorname{diam}(\mathcal{B}_k) = \max_{B \in \mathcal{B}_k} \operatorname{diam}(B)$$

converges to zero for $k \to \infty$. Given an initial collection $\mathcal{B}_0$, we inductively obtain $\mathcal{B}_k$ from $\mathcal{B}_{k-1}$ for $k = 1, 2, \ldots$ in two steps:

(i) *Subdivision:* Construct a new collection $\hat{\mathcal{B}}_k$ such that

$$\bigcup_{B \in \hat{\mathcal{B}}_k} B = \bigcup_{B \in \mathcal{B}_{k-1}} B \tag{2.3}$$

and

$$\operatorname{diam}(\hat{\mathcal{B}}_k) \leq \theta_k \operatorname{diam}(\mathcal{B}_{k-1}), \tag{2.4}$$

where $0 < \theta_{\min} \leq \theta_k \leq \theta_{\max} < 1$.

(ii) *Selection:* Define the new collection $\mathcal{B}_k$ by

$$\mathcal{B}_k = \left\{ B \in \hat{\mathcal{B}}_k : \exists \hat{B} \in \hat{\mathcal{B}}_k \text{ such that } f^{-1}(B) \cap \hat{B} \neq \emptyset \right\}. \tag{2.5}$$

By construction

$$\operatorname{diam}(\mathcal{B}_k) \leq \theta_{\max}^k \operatorname{diam}(\mathcal{B}_0) \to 0 \quad \text{for } k \to \infty.$$

EXAMPLE 2.5 We consider $f : \mathbb{R} \to \mathbb{R}$,

$$f(x) = \alpha x,$$

where $\alpha \in (0, \frac{1}{2})$ is a constant. Then the global attractor $A = \{0\}$ of f is a stable fixed point. We begin the subdivision procedure with $\mathcal{B}_0 = \{[-1, 1]\}$ and construct $\hat{\mathcal{B}}_k$ by bisection. In the first subdivision step we obtain

$$\mathcal{B}_1 = \hat{\mathcal{B}}_1 = \{[-1, 0], [0, 1]\}.$$

No interval is removed in the selection step, since each of them is mapped into itself. Now subdivision leads to

$$\hat{\mathcal{B}}_2 = \left\{ [-1, -\frac{1}{2}], [-\frac{1}{2}, 0], [0, \frac{1}{2}], [\frac{1}{2}, 1] \right\}.$$

Applying the selection rule (2.5), the two boundary intervals are removed, i.e.

$$\mathcal{B}_2 = \left\{ [-\frac{1}{2}, 0], [0, \frac{1}{2}] \right\}.$$

Proceeding this way, we obtain after k subdivision steps

$$\mathcal{B}_k = \left\{ [-\frac{1}{2^{k-1}}, 0], [0, \frac{1}{2^{k-1}}] \right\}.$$

We see that the union $\bigcup_{B \in \mathcal{B}_k} B$ is indeed approaching the global attractor $A = \{0\}$ for $k \to \infty$. The speed of convergence obviously depends on the contraction rate of the global attractor. We will come back to this observation in Subsection 2.3.

Convergence Result

The abstract subdivision algorithm does converge to the relative global attractor A_Q. In fact for the nested sequence of sets

$$Q_k = \bigcup_{B \in \mathcal{B}_k} B, \quad k = 0, 1, 2, \ldots, \tag{2.6}$$

one can show the following result (see Dellnitz and Hohmann (1997)).

PROPOSITION 2.6 *Let A_Q be a global attractor relative to the compact set Q, and let $\mathcal{B}_0$ be a finite collection of closed subsets with $Q_0 = \bigcup_{B \in \mathcal{B}_0} B = Q$. Then*

$$\lim_{k \to \infty} h\left(A_Q, Q_k\right) = 0,$$

where $h(B, C)$ denotes the usual Hausdorff distance between two compact subsets $B, C \subset \mathbb{R}^n$.

2.3 Convergence Behavior and Error Estimate

We begin by recalling the definition of a hyperbolic set (see e.g. Shub (1987)).

DEFINITION 2.7 Let Λ be an invariant set for the diffeomorphism f. We say that Λ is a *hyperbolic set* for f if there is a continuous invariant splitting $T_\Lambda \mathbb{R}^n = E^s_\Lambda \oplus E^u_\Lambda$,

$$Df(E^s_x) = E^s_{f(x)} \quad \text{and} \quad Df(E^u_x) = E^u_{f(x)},$$

for which there are constants $c > 0$ and $\lambda \in (0,1)$, such that

a) if $v \in E^s_x$, then $\|Df^j(x)v\| \leq c\lambda^j \|v\|$ for all $j \in \mathbb{N}$;

b) if $v \in E^u_x$, then $\|Df^{-j}(x)v\| \leq c\lambda^j \|v\|$ for all $j \in \mathbb{N}$.

Since the estimates in Definition 2.7 are formulated in terms of the Jacobians, they are just valid infinitesimally for f. A consideration of the asymptotic behavior with respect to the diffeomorphism f itself leads to the definition of *stable* and *unstable manifolds*.

DEFINITION 2.8 For $x \in \mathbb{R}^n$ and $\epsilon > 0$ we define the *local stable (unstable) manifold* by

$$\begin{aligned} W^s_\epsilon(x) &= \{y \in \mathbb{R}^n : d(f^j(x), f^j(y)) \to 0 \text{ for } j \to \infty \\ &\qquad \text{and } d(f^j(x), f^j(y)) \leq \epsilon \text{ for all } j \geq 0\}, \\ W^u_\epsilon(x) &= \{y \in \mathbb{R}^n : d(f^j(x), f^j(y)) \to 0 \text{ for } j \to -\infty \\ &\qquad \text{and } d(f^j(x), f^j(y)) \leq \epsilon \text{ for all } j \leq 0\}. \end{aligned}$$

We now state part of the results which are known as the *Stable Manifold Theorem* for hyperbolic sets. A proof can be found in e.g. Shub (1987).

THEOREM 2.9 *Let Λ be a closed hyperbolic set for f. Then there is a positive ϵ such that for every point $x \in \Lambda$, $W^s_\epsilon(x)$ and $W^u_\epsilon(x)$ are embedded disks of dimension equal to those of E^s_x and E^u_x respectively. The tangent space of $W^s_\epsilon(x)$ ($W^u_\epsilon(x)$) at x is E^s_x (E^u_x).*

Moreover, $W^s_\epsilon(x)$ and $W^u_\epsilon(x)$ satisfy the following properties:

(i) There is a constant $C > 0$ such that

$$\begin{aligned} d(f^j(x), f^j(y)) &\leq C\lambda^j d(x,y) \quad \textit{for all } y \in W^s_\epsilon(x) \textit{ and } j \geq 0, \\ d(f^{-j}(x), f^{-j}(y)) &\leq C\lambda^j d(x,y) \quad \textit{for all } y \in W^u_\epsilon(x) \textit{ and } j \geq 0, \end{aligned}$$

where λ is chosen according to Definition 2.7.

(ii) The local stable and unstable manifolds are given by

$$\begin{aligned} W^s_\epsilon(x) &= \{y \in \mathbb{R}^n : d(f^j(x), f^j(y)) \le \epsilon \text{ for all } j \ge 0\}, \\ W^u_\epsilon(x) &= \{y \in \mathbb{R}^n : d(f^j(x), f^j(y)) \le \epsilon \text{ for all } j \le 0\}. \end{aligned}$$

We may use Theorem 2.9 to obtain a result on the convergence behavior of the subdivision algorithm in the case where the relative global attractor is part of an attracting compact hyperbolic set A. Define for $\sigma > 0$

$$U_\sigma(A) = \{y \in \mathbb{R}^n : \text{if } y \in W^s(x),\, x \in A, \text{ then } d(x, y) < \sigma\}.$$

Obviously, A is a subset of $U_\sigma(A)$. In the following result we assume for simplicity that $\mathcal{B}_0 = \{Q\}$. A proof can be found in Dellnitz and Hohmann (1997).

PROPOSITION 2.10 *Let A_Q be a global attractor of the diffeomorphism f^q relative to the closed set Q, and suppose that A_Q is an attracting compact hyperbolic set of f. Let $\rho \ge 1$ be a constant such that for each compact neighborhood $\widetilde{Q}$ of A_Q we have*

$$h(A_Q, \widetilde{Q}) \le \delta \Longrightarrow \widetilde{Q} \subset U_{\rho\delta}(A_Q). \tag{2.7}$$

Then the coverings Q_k obtained by the subdivision algorithm for f^q satisfy

$$h(A_Q, Q_k) \le \operatorname{diam}(\mathcal{B}_k)(1 + \alpha + \alpha^2 + \cdots + \alpha^k), \tag{2.8}$$

where $\alpha = C\rho\lambda^q/\theta_{\min}$ and C, λ are the characteristic constants of the underlying hyperbolic set (see Theorem 2.9).

REMARKS 2.11 (a) Geometrically it is evident that close to A_Q both constants C and ρ are of order one.

(b) Recently the estimate on $h(A_Q, Q_k)$ in Proposition 2.10 has been used to develop an efficient global zero finding procedure (see Dellnitz et al. (2000c)). There the underlying idea is to view iteration schemes such as Newton's method as specific dynamical systems.

COROLLARY 2.12 *If the power q is chosen such that*

$$\alpha = \frac{C\rho\lambda^q}{\theta_{\min}} < 1,$$

then we have for all k

$$h(A_Q, Q_k) \le \frac{1}{1-\alpha} \operatorname{diam}(\mathcal{B}_k).$$

2.4 Numerical Examples

EXAMPLE 2.13 We begin by considering a two dimensional dynamical system, the (scaled) Hénon map

$$f(x) = \begin{pmatrix} 1 - ax_1^2 + x_2/5 \\ 5bx_1 \end{pmatrix}. \tag{2.9}$$

The computations are performed with $b = 0.2$ and $a = 1.2$. Starting with the square $[-2, 2]^2$, we display in Figure 1 the coverings obtained by the algorithm after $k = 6, 8, 10, 12$ subdivision steps. For details concerning the implementation of the algorithm see Section 8. In Figure 2(a) we show the rectangles covering the relative global attractor after 18 subdivision steps. After this number of steps the diameter of the boxes is already 0.011.

We remark that a direct simulation would not yield the same result. In Figure 2(b) we illustrate this fact by showing the attractor that appears if the transient behavior has been neglected. The reason for the difference lies in the fact that the subdivision algorithm covers all invariant sets in $[-2, 2]^2$ – together with their unstable manifolds. In particular, the one-dimensional unstable manifolds of the two fixed points (marked with circles in Figure 2(b)) are approximated – but those cannot be computed by direct simulation.

EXAMPLE 2.14 In this example we consider the following system of first order ordinary differential equations known as *Chua's circuit*,

$$\begin{aligned} \dot{x} &= \alpha(y - m_0 x - \frac{1}{3} m_1 x^3) \\ \dot{y} &= x - y + z \\ \dot{z} &= -\beta y. \end{aligned}$$

In the computations we have chosen $\alpha = 18$, $\beta = 33$, $m_0 = -0.2$ and $m_1 = 0.01$. We consider the diffeomorphism f given by the corresponding time-one-map, and approximate the relative global attractor inside $Q = [-12, 12] \times [-2.5, 2.5] \times [-20, 20]$. The results of the subdivision algorithm for $k = 8, 11, 20$ steps are displayed in Figure 3. In this figure we also show an approximation of the attractor obtained by direct simulation. With each of the set oriented computations we have covered the union of the global unstable manifolds of the three steady state solutions contained in Q. Again we refer to Section 8 for the details concerning the implementation of the subdivision algorithm.

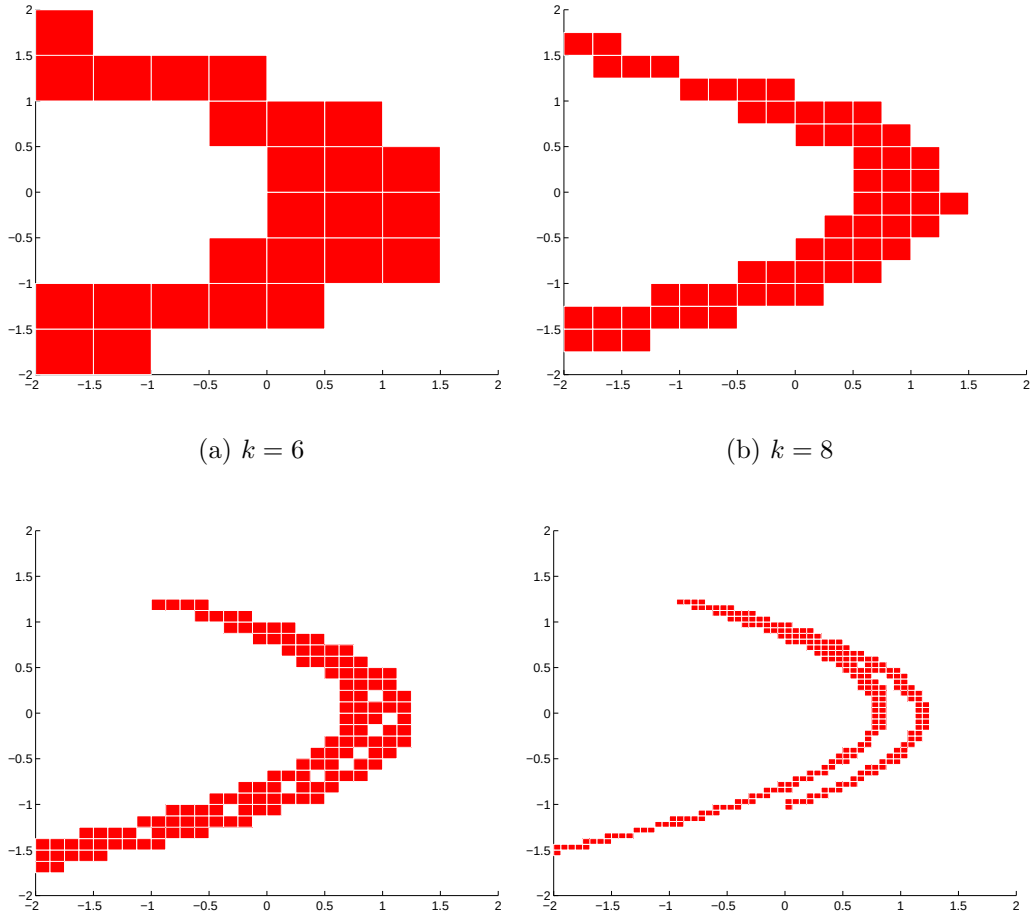

(a) $k = 6$ (b) $k = 8$

(c) $k = 10$ (d) $k = 12$

Figure 1: Successively finer coverings of the global Hénon attractor.

2.5 The Computation of Chain Recurrent Sets

The subdivision algorithm can easily be modified in such a way that one can approximate the chain recurrent set within a given compact set $Q \subset \mathbb{R}^n$. Again we construct a sequence $\mathcal{B}_0, \mathcal{B}_1, \ldots$ of finite collections of compact subsets of Q creating successively tighter coverings of the desired object.

Set $\mathcal{B}_0 = \{Q\}$. For $k = 1, 2, \ldots$ the collection $\mathcal{B}_k$ is obtained from $\mathcal{B}_{k-1}$ in two steps:

(i) *Subdivision:* Subdivide each set in the current collection $\mathcal{B}_{k-1}$ into sets of smaller diameter;

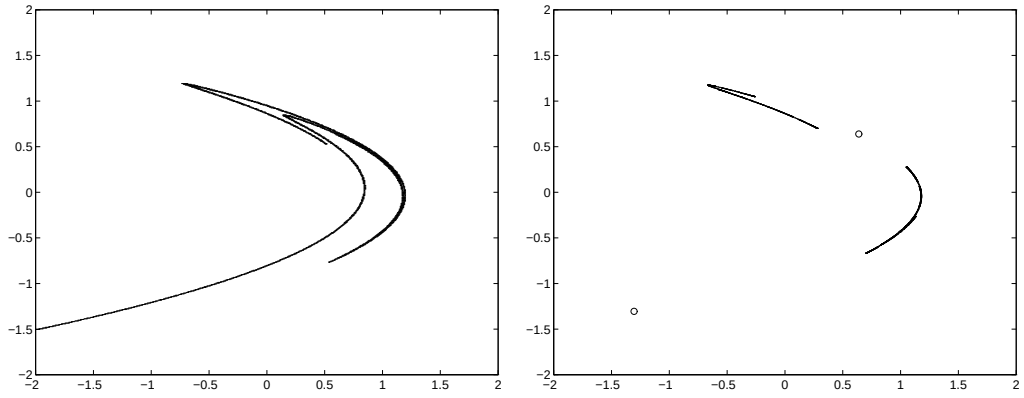

(a) Subdivision (b) Simulation

Figure 2: (a) Approximation of the relative global attractor for the Hénon mapping after 18 subdivision steps; (b) attractor of the Hénon mapping computed by direct simulation. The two fixed points are marked with ∘.

(ii) *Selection:* Construct a directed graph whose vertices are the sets in the refined collection and by defining an edge from vertex B to vertex B', if

$$f(B) \cap B' \neq \emptyset. \tag{2.10}$$

Compute the strongly connected components of this graph and discard all sets of the refined collection which are not contained in one of these components.

REMARK 2.15 Recall that a subset W of the nodes of a directed graph is called a *strongly connected component* of the graph, if for all $w, \tilde{w} \in W$ there is a path from w to $\tilde{w}$. The set of all strongly connected components of a given directed graph can be computed in linear time (Mehlhorn (1984)).

Intuitively it is plausible that the sequence of box coverings $\mathcal{B}_k$ converges to the chain recurrent set of f. Indeed, under mild assumptions on the box coverings one can prove convergence, see Eidenschink (1995); Osipenko (1999).

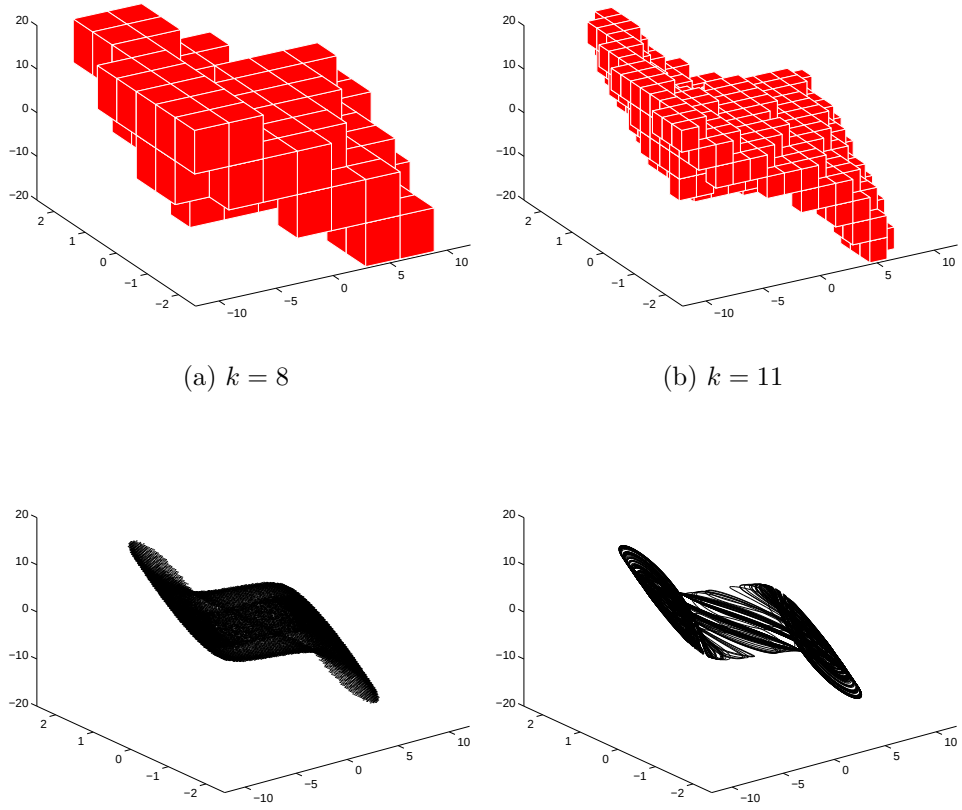

(a) $k = 8$ (b) $k = 11$

(c) $k = 20$ (d) Simulation

Figure 3: (a)-(c) Successively finer coverings of a relative global attractor for Chua's circuit; (d) approximation obtained by direct simulation.

2.6 Numerical Example

We consider the following scenario and conclusion – the latter one is an application of the Wazewski Theorem – which goes back to Conley (1978):

> Let φ^t denote a flow of an ordinary differential equation on $\mathbb{R}^3$ with the following properties: there is a cylinder of finite length such that outside the cylinder trajectories run vertically downward with respect to the cylinder. Assume further that there is some solution running through the cylinder which makes a knot as it goes from top to bottom. Then there must be a nontrivial invariant set inside the cylinder.

Using the subdivision algorithm described above one can compute a covering of the chain recurrent set in the cylinder – see Dellnitz et al. (2000b) for details on how to explicitly construct the vector field with the desired properties.

Figure 4, which has been produced together with Martin Rumpf and Robert Strzodka (both University of Bonn), shows the knotted trajectory and a covering of the chain recurrent set in blue after 30 subdivision steps.

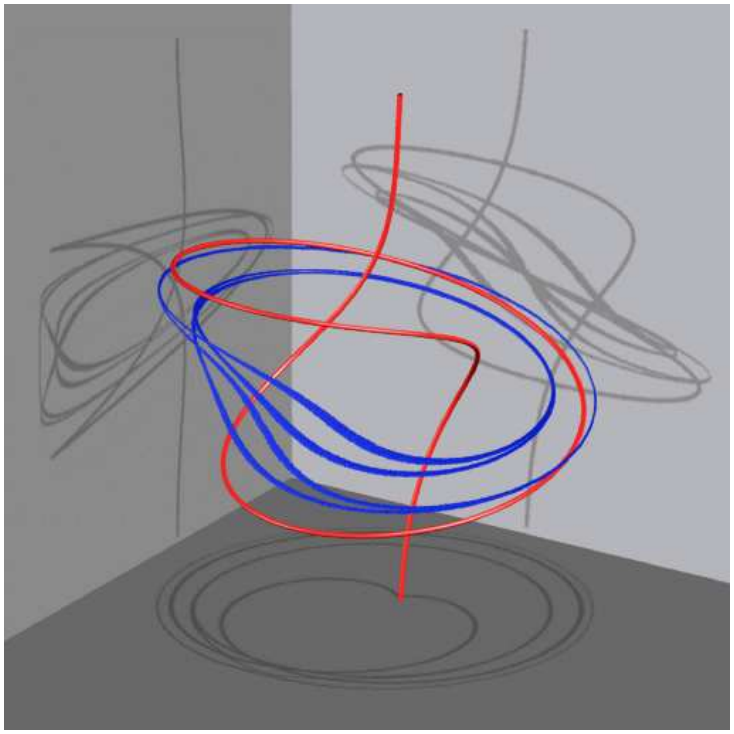

Figure 4: Invariant set in a knotted flow. The covering of the chain recurrent set is shown in blue. The knotted trajectory that defines the flow is colored red.

3 The Computation of Invariant Manifolds

We now present a set oriented method for the computation of invariant manifolds. Although the method can in principle be applied to manifolds of arbitrary hyperbolic invariant sets we will restrict, for simplicity, to the case where the underlying invariant set of (2.1) is a hyperbolic fixed point.

3.1 Description of the Method

The continuation starts at a hyperbolic fixed point p with the unstable manifold $W^u(p)$. We fix once and for all a (large) compact set $Q \subset \mathbb{R}^n$ containing p, in which we want to approximate part of $W^u(p)$. To combine the subdivision process with a continuation method, we realize the subdivision using a family of partitions of Q. A *partition* $\mathcal{P}$ of Q consists of finitely many subsets of Q such that

$$\bigcup_{B \in \mathcal{P}} B = Q \quad \text{and} \quad B \cap B' = \emptyset \quad \text{for all } B, B' \in \mathcal{P} \text{ with } B \neq B'.$$

Let $\mathcal{P}_\ell$, $\ell \in \mathbb{N}$, be a nested sequence of successively finer partitions of Q, requiring that for all $B \in \mathcal{P}_\ell$ there exist $B_1, \ldots, B_m \in \mathcal{P}_{\ell+1}$ such that $B = \bigcup_i B_i$ and $\operatorname{diam}(B_i) \leq \theta \operatorname{diam}(B)$ for some $0 < \theta < 1$. A set $B \in \mathcal{P}_\ell$ is said to be of *level* ℓ.

Let $C \in \mathcal{P}_\ell$ be a neighborhood of the hyperbolic fixed point p such that the global attractor relative to C satisfies

$$A_C = W^u_{\mathrm{loc}}(p) \cap C.$$

Applying the subdivision algorithm with k subdivision steps to $\mathcal{B}_0 = \{C\}$, we obtain a covering $\mathcal{B}_k \subset \mathcal{P}_{\ell+k}$ of the local unstable manifold $W^u_{\mathrm{loc}}(p) \cap C$, that is,

$$A_C = W^u_{\mathrm{loc}}(p) \cap C \subset \bigcup_{B \in \mathcal{B}_k} B. \tag{3.1}$$

By Proposition 2.6, this covering converges to $W^u_{\mathrm{loc}}(p) \cap C$ for $k \to \infty$.

Continuation Method

We are now in the position to describe a continuation algorithm for the approximation of unstable manifolds. For a fixed k we define a sequence $\mathcal{C}_0^{(k)}, \mathcal{C}_1^{(k)}, \ldots$ of subsets $\mathcal{C}_j^{(k)} \subset \mathcal{P}_{\ell+k}$ by

(i) *Initialization:*

$$\mathcal{C}_0^{(k)} = \mathcal{B}_k.$$

(ii) *Continuation:* For $j = 0, 1, 2, \ldots$ define

$$\mathcal{C}_{j+1}^{(k)} = \left\{ B \in \mathcal{P}_{\ell+k} \ : \ B \cap f(B') \neq \emptyset \text{ for some } B' \in \mathcal{C}_j^{(k)} \right\}.$$

Observe that the sets

$$C_j^{(k)} = \bigcup_{B \in \mathcal{C}_j^{(k)}} B$$

form nested sequences in k, i.e.,

$$C_j^{(0)} \supset C_j^{(1)} \supset \ldots \text{ for } j = 0, 1, 2, \ldots.$$

3.2 Convergence Behavior and Error Estimate

Convergence Result

Set $W_0 = W^u_{\text{loc}}(p) \cap C$ and define inductively for $j = 0, 1, 2, \ldots$

$$W_{j+1} = f(W_j) \cap Q.$$

Then it is not too difficult to prove the following convergence result (see Dellnitz and Hohmann (1996)).

PROPOSITION 3.1 *The sets $C_j^{(k)}$ are coverings of W_j for all $j, k = 0, 1, \ldots$. Moreover, for fixed j, $C_j^{(k)}$ converges to W_j in Hausdorff distance if the number k of subdivision steps in the initialization goes to infinity.*

It can in general not be guaranteed that the continuation method leads to an approximation of the entire set $W^u(p) \cap Q$. The reason is that the unstable manifold of the hyperbolic fixed point p may "leave" Q but may as well "wind back" into it. If this is the case then it can indeed happen that the continuation method, as described above, will not cover all of $W^u(p) \cap Q$.

Error Estimate

Observe that the convergence result in Proposition 3.1 does not require the existence of a hyperbolic structure along the unstable manifold. However, if we additionally assume its existence then we can establish results on the convergence behavior of the continuation method in a completely analogous way as in Dellnitz and Hohmann (1997).

To this end assume that p is an element of an attractive hyperbolic set A. Then the unstable manifold of p is contained in A. Choose

$$Q = \overline{\bigcup_{x \in A} W^s_\eta(x)}$$

for some sufficiently small $\eta > 0$. Note that $A = A_Q$. As in (2.7) let $\rho \geq 1$ be a constant such that for every compact neighborhood $\widetilde{Q} \subset Q$ of A_Q we have

$$h(A_Q, \widetilde{Q}) \leq \delta \quad \Rightarrow \quad \widetilde{Q} \subset U_{\rho\delta}(A_Q). \tag{3.2}$$

A proof of the following result can be found in Junge (1999).

PROPOSITION 3.2 *Assume that in the initialization step of the continuation method we have*

$$h(W_0, C_0^{(k)}) \leq \zeta \operatorname{diam} \mathcal{C}_0^{(k)}$$

for some constant $\zeta > 0$. *If* $C_j^{(k)} \subset W_\eta^s(W_j)$ *for* $j = 0, 1, 2, \ldots, J$, *then*

$$h(W_j, C_j^{(k)}) \leq \operatorname{diam} \mathcal{C}_j^{(k)} \max\left(\zeta, 1 + \beta + \beta^2 + \cdots + \beta^j \zeta\right) \tag{3.3}$$

for $j = 1, 2, \ldots, J$. *Here* $\beta = C\lambda\rho$ *and* C *and* λ *are the characteristic constants of the hyperbolic set* A *(see Theorem 2.9).*

The estimate (3.3) points up the fact that for a given initial level k and λ near 1 – corresponding to a weak contraction transversal to the unstable manifold – the approximation error may increase dramatically with an increasing number of continuations steps (increasing j).

3.3 Numerical Examples

EXAMPLE 3.3 As the first example we compute an approximation of a two-dimensional stable manifold of the origin in the Lorenz system

$$\begin{aligned} \dot{x} &= \sigma(y - x) \\ \dot{y} &= \rho x - y - xz \\ \dot{z} &= -\beta z + xy. \end{aligned}$$

In this computation we have chosen the "standard" set of parameter values, that is $\sigma = 10, \rho = 28$ and $\beta = 8/3$. With this choice a direct numerical simulation would lead to an approximation of the celebrated Lorenz attractor. (For illustrations as well as a discussion of topological properties of the Lorenz attractor the reader is referred to Guckenheimer and Holmes (1983).)

Since we want to compute the two-dimensional stable manifold of the origin, we proceed backwards in time and apply the continuation method to the diffeomorphism given by the time-$(-T)$-map. Starting in a neighborhood of $(0, 0, 0)$ we approximate the stable manifold inside $Q = [-25, 25]^3$.

To demonstrate the continuation process, we begin with a rough approximation using the initial level $\ell = 9$ and $k = 3$ subdivision steps. In Figure 5 we display the coverings obtained by the algorithm after $j = 0, 1, 3$ and 5 continuation steps. We remark that in this case the stable eigenvalues are both

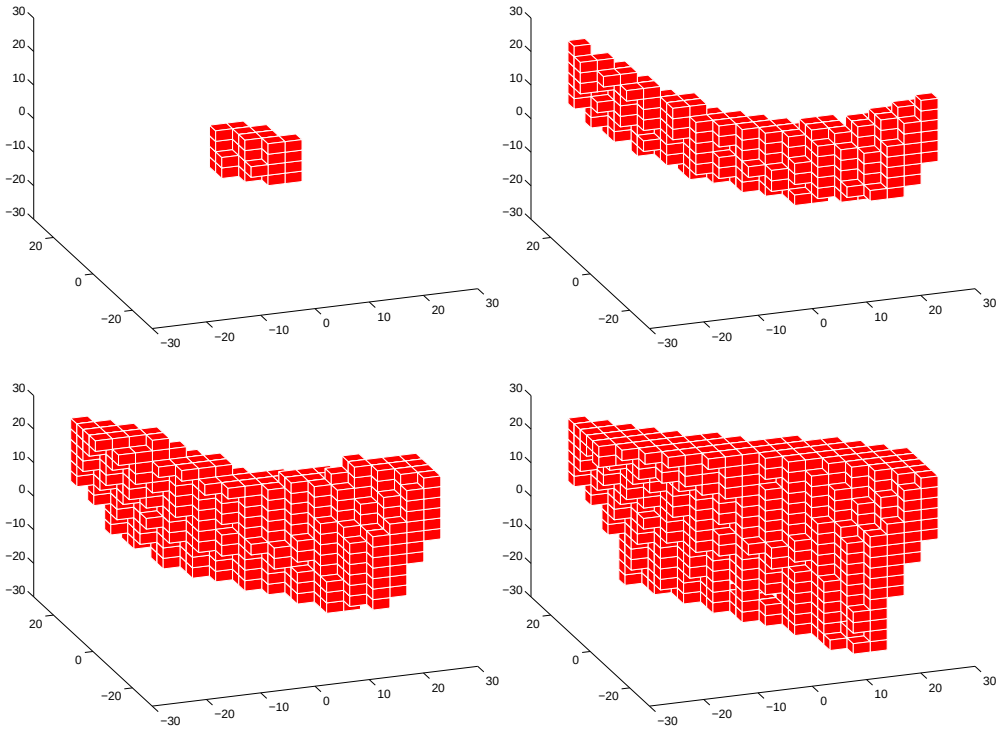

Figure 5: Continuation steps for the stable manifold of the origin in the Lorenz system for $j = 0, 1, 3, 5$.

real but the ratio of strong and weak contraction is relatively large. This is also reflected by the way the covering is growing (see Figure 5). A finer resolution ($\ell = 21, k = 0$, 10 steps, $Q = [-120, 120] \times [-120, 120] \times [-160, 160]$) is shown in Figure 6.

EXAMPLE 3.4 As the second example let us consider a Hamiltonian system, the Circular Restricted Three Body Problem. Its equations of motion in a rotating frame are given by

$$\begin{aligned} \dot{x} &= u, & \dot{u} &= 2v + x + c_1(x + \mu - 1) + c_2(x + \mu), \\ \dot{y} &= v, & \dot{v} &= -2u + y + (c_1 + c_2)y, \\ \dot{z} &= w, & \dot{w} &= (c_1 + c_2)z, \end{aligned} \tag{3.4}$$

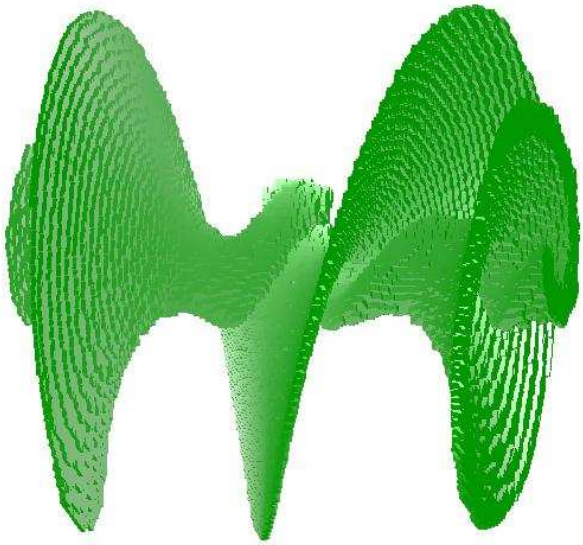

Figure 6: Covering of the two-dimensional stable manifold of the origin in the Lorenz system.

where

$$c_1 = -\frac{\mu}{((x+\mu-1)^2+y^2+z^2)^{\frac{3}{2}}}, \quad c_2 = -\frac{1-\mu}{((x+\mu)^2+y^2+z^2)^{\frac{3}{2}}}$$

and $\mu = m_1/(m_1+m_2)$ is the normalized mass of one of the primary bodies. We use the value $\mu = 3.040423398444176 \cdot 10^{-6}$ for the sun/earth system here.

We aim for the computation of the unstable manifold of a certain unstable periodic orbit. As it was pointed out in the error estimates in Section 3.2 a naive application of the continuation method would – due to the Hamiltonian nature of the system – not lead to satisfactory results in this case. We therefore apply a modified version of this method, see Junge (1999). Roughly speaking the idea is not to continue the current covering by considering *one* application of the map at *each* continuation step, but instead to perform only *one* continuation step while computing *several* iterates of the map.

More formally, we replace the second step in the continuation method by:

(ii) *Continuation:* For some $J > 0$ define

$$\mathcal{C}_J^{(k)} = \left\{ B \in \mathcal{P}_{\ell+k} \ : \ \exists\, 0 \le j \le J : B \cap f^j(B') \neq \emptyset \text{ for some } B' \in \mathcal{C}_0^{(k)} \right\}.$$

The convergence statement in Proposition 3.1 is adapted to this method in a straightforward manner. One can also show that – as intended – the Hausdorff-distance between compact parts of the unstable manifold and the computed covering is of the order of the diameter of the partition, see Junge (1999) for details. However, and this is the price one has to pay, one no longer considers short term trajectories here and therefore accumulates methodological and round-off errors when computing the iterates f^j.

A second advantage of the modified continuation method is that whenever the given dynamical system stems from a flow ϕ^t one can get rid of the necessity to consider a time-T-map and instead replace the continuation step by

(ii) *Continuation:* For some $T > 0$ define

$$\mathcal{C}_T^{(k)} = \left\{ B \in \mathcal{P}_{\ell+k} \ : \ \exists\, 0 \le t \le T : B \cap \phi^t(B') \neq \emptyset \text{ for some } B' \in \mathcal{C}_0^{(k)} \right\}.$$

This facilitates the usage of integrators with adaptive step-size control and finally made the computations for the Restricted Three Body Problem feasible. Figure 7 shows the result of the computation, where we set $T = 7$ and used an embedded Runge-Kutta scheme of order 8(7) (see Dormand and Prince (1981)) with error tolerances set to 10^{-9}. See again Junge (1999) for more details on this computation.

4 The Computation of SRB-Measures

An important statistical characterization of the behavior of a dynamical system is given by so-called *SRB (Sinai-Ruelle-Bowen)* measures. The important property of these invariant measures is, roughly speaking, that they lend weight to a region in phase space according to the probability by which "typical" trajectories visit this region. In this section we present a set oriented numerical method for the approximation of SRB-measures.

The main idea of the approach is to define an operator (the *Perron-Frobenius operator*) on the space of probability measures whose fixed points

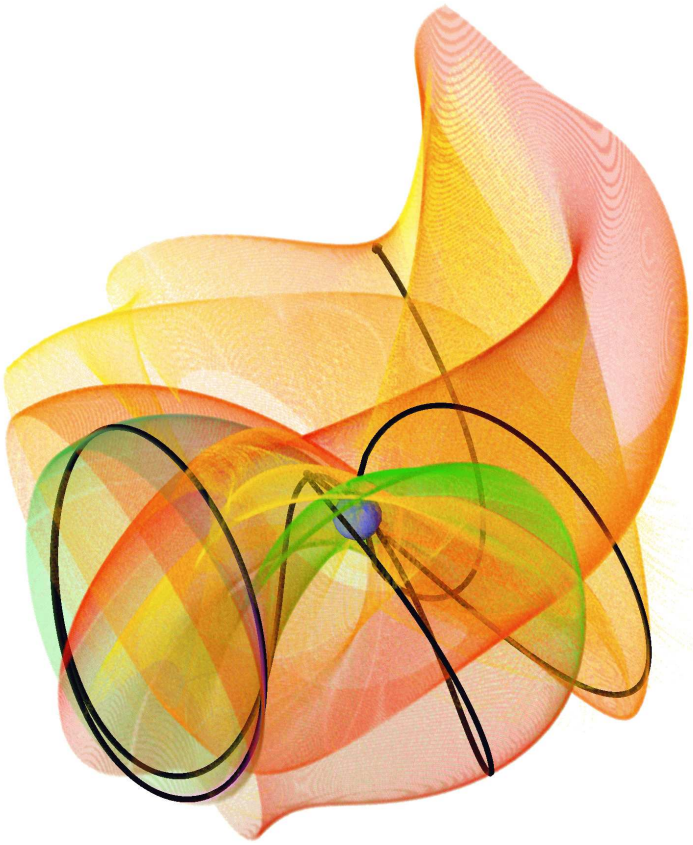

Figure 7: Covering of part of the global unstable manifold of an unstable periodic orbit in the Circular Restricted Three Body Problem. The blue body depicts the earth, the black trajectory is a sample orbit which leaves the periodic orbit in the direction of the earth.

are invariant measures, then to discretize this operator via a Galerkin method and finally to compute fixed points of the resulting matrix as an approximation to an invariant measure. Using spaces of piecewise constant functions on a partition of the underlying phase space this approach is commonly known as "Ulam's method", see Ulam (1960). There exist various statements about the convergence properties of Ulam's method, see e.g. Li (1976); G. Keller (1982); Ding et al. (1993); Ding and Zhou (1996); Froyland (1996). In the following sections we are going to establish a convergence result for uniformly hyperbolic systems by combining a theorem of Kifer (1986) on the stochastic stability of SRB-measures with results on the spectral approximation of compact operators.

4.1 Brief Review on SRB-Measures and Small Random Perturbations

Our aim is to obtain information about the statistical behavior of (deterministic) discrete dynamical systems of the form (2.1) where $f : X \to X$ is a diffeomorphism on a compact subset $X \subset \mathbb{R}^n$.

SRB-Measures

We denote by $\mathcal{B}$ the Borel σ–Algebra on X and by m the Lebesgue measure on $\mathcal{B}$. Moreover, let $\mathcal{M}$ be the space of probability measures on $\mathcal{B}$. Recall that a measure $\mu \in \mathcal{M}$ is *invariant* if

$$\mu(B) = \mu(f^{-1}(B)) \quad \text{for all } B \in \mathcal{B}.$$

An invariant measure μ is *ergodic* if

$$\mu(C) \in \{0, 1\} \quad \text{for all invariant sets } C \in \mathcal{B}.$$

Now we recall the notion of an SRB-measure. There exist several equivalent definitions in the situation where the underlying dynamical behavior is Axiom A, and we state one of them.

Definition 4.1 An ergodic measure μ is an *SRB-measure* if there exists a subset $U \subset X$ with $m(U) > 0$ and such that for each continuous function ψ

$$\lim_{N\to\infty} \frac{1}{N} \sum_{j=0}^{N-1} \psi(f^j(x)) = \int \psi \, d\mu \tag{4.1}$$

for all $x \in U$.

Remarks 4.2 (a) Recall that (4.1) always holds for μ-a.e. $x \in X$ by the Birkhoff Ergodic Theorem. The crucial difference for an SRB-measure is that the temporal average equals the spatial average for a set of initial points $x \in X$ which has positive Lebesgue-measure. This is the reason why this measure is also referred to as the *natural* or the *physically relevant* invariant measure.

(b) The concept of SRB-measures in the context of Anosov systems has been introduced by Y.G. Sinai in the 1960's (e.g. Sinai (1972)). Later

the existence of SRB-measures has been shown for Axiom A systems by R. Bowen and D. Ruelle (see Ruelle (1976); Bowen and Ruelle (1975)). It should be mentioned as well that also Lasota and Yorke have proved the existence of these measures for a particular class of interval maps already in 1973, Lasota and Yorke (1973). M. Benedicks and L.-S. Young have shown that the Hénon map has an SRB-measure for a "large" set of parameter values, Benedicks and Young (1993). More recently, Tucker proved the existence of an SRB-measure for the Lorenz system, Tucker (1999).

Stochastic Transition Functions

Although our aim is to consider deterministic systems it turns out to be more convenient to consider the stochastic context first.

DEFINITION 4.3 A function $p : X \times \mathcal{B} \to [0,1]$ is a *stochastic transition function*, if

(i) $p(x, \cdot)$ is a probability measure for every $x \in X$,

(ii) $p(\cdot, A)$ is Lebesgue-measurable for every $A \in \mathcal{B}$.

Let δ_y denote the Dirac measure supported on the point $y \in X$. Then $p(x, A) = \delta_{h(x)}(A)$ is a stochastic transition function for every m-measurable function h. We will see below that the specific choice $h = f$ represents the deterministic situation in this more general set-up.

We now define the notion of an invariant measure in the stochastic setting.

DEFINITION 4.4 Let p be a stochastic transition function. If $\mu \in \mathcal{M}$ satisfies

$$\mu(A) = \int p(x, A)\, d\mu(x)$$

for all $A \in \mathcal{B}$, then μ is an *invariant measure of* p.

The following example illustrates the previous remark that we recover the deterministic situation in the case where $p(x, \cdot) = \delta_{f(x)}$.

EXAMPLE 4.5 Suppose that $p(x, \cdot) = \delta_{f(x)}$ and let μ be an invariant measure of p. Then we compute for $A \in \mathcal{B}$

$$\mu(A) = \int p(x, A)\, d\mu(x) = \int \delta_{f(x)}(A)\, d\mu(x) = \int \chi_A(f(x))\, d\mu(x) = \mu(f^{-1}(A)),$$

where we denote by χ_A the characteristic function of A. Thus, μ is an invariant measure for the diffeomorphism f.

Small Random Perturbations

Now we assume that for every $x \in X$ the probability measure $p(x, \cdot)$ is absolutely continuous with respect to the Lebesgue measure m. Hence we may write $p(x, \cdot)$ as

$$p(x, A) = \int_A k(x, y)\, dm(y) \quad \text{for all } A \in \mathcal{B},$$

with an appropriate *transition density function* $k : X \times X \to \mathbb{R}$. Obviously,

$$k(x, \cdot) \in L^1(X, m) \quad \text{and} \quad k(x, y) \geq 0.$$

In this case we also call the stochastic transition function p *absolutely continuous*. Note that

$$\int k(x, y)\, dm(y) = p(x, X) = 1 \quad \text{for all } x \in X.$$

We now specify concretely the stochastic transition function p which is the theoretical tool for the derivation of a convergence result to SRB-measures. Recall that the purpose is to approximate the SRB-measure of a *deterministic* dynamical system represented by a diffeomorphism f. Hence the *stochastic* system that we consider should be a small perturbation of this original deterministic system.

For $\varepsilon > 0$ we set

$$k_\varepsilon(x, y) = \frac{1}{\varepsilon^n m(B)} \chi_B \left(\frac{1}{\varepsilon} \Big(y - x \Big) \right), \quad x, y \in X. \tag{4.2}$$

Here $B = B_0(1)$ denotes the open ball in $\mathbb{R}^n$ of radius one and χ_B is the characteristic function of B. Obviously $k_\varepsilon(f(x), y)$ is a transition density function and we may define a stochastic transition function p_ε by

$$p_\varepsilon(x, A) = \int_A k_\varepsilon(f(x), y)\, dm(y). \tag{4.3}$$

REMARK 4.6 Note that $p_\varepsilon(x, \cdot) \to \delta_{f(x)}$ for $\varepsilon \to 0$ uniformly in x in a weak*–sense. Hence the Markov process defined by any initial probability measure μ and the transition function p_ε is a *small random perturbation* of the deterministic system f in the sense of Kifer (1986).

4.2 Spectral Approximation for the Perron-Frobenius Operator

The main purpose of this section is to describe an appropriate Galerkin method for the approximation of a specific type of transfer operator, namely the *Perron-Frobenius operator*. This operator is used for translating the problem of finding an invariant measure into a fixed point problem.

The Perron-Frobenius Operator

DEFINITION 4.7 Let p be a stochastic transition function. Then the *Perron-Frobenius operator* $P : \mathcal{M}_{\mathbb{C}} \to \mathcal{M}_{\mathbb{C}}$ is defined by

$$P\mu(A) = \int p(x, A)\, d\mu(x),$$

where $\mathcal{M}_{\mathbb{C}}$ is the space of bounded complex valued measures on $\mathcal{B}$. If p is absolutely continuous with density function k then we may define the Perron-Frobenius operator P on L^1 by

$$Pg(y) = \int k(x, y)g(x)\, dm(x) \quad \text{for all } g \in L^1.$$

REMARKS 4.8 (a) By definition a measure $\mu \in \mathcal{M}$ is invariant if and only if it is a fixed point of P. In other words, invariant measures correspond to eigenmeasures of P for the eigenvalue one.

Moreover, let $\lambda \in \mathbb{C}$ be an eigenvalue of P with corresponding eigenmeasure ν, that is, $P\nu = \lambda\nu$. Then in particular

$$\lambda\nu(X) = P\nu(X) = \int p(x, X)\, d\nu(x) = \nu(X)$$

since $p(x, X) = 1$ for all $x \in X$. It follows that $\nu(X) = 0$ if $\lambda \neq 1$.

(b) Observe that in the deterministic situation where $p(x, \cdot) = \delta_{f(x)}$ we obtain

$$P\mu(A) = \int p(x, A)\, d\mu(x) = \mu(f^{-1}(A))$$

(cf. Example 4.5). This is indeed the standard definition of the Perron-Frobenius operator in the deterministic setting (see e.g. Lasota and Mackey (1994)).

Spectral information for the Perron-Frobenius operator cannot just be used for the approximation of SRB-measures but also for the identification of cyclic dynamical behavior, that is, there exist finitely many different compact subsets in state space which are cyclically permuted by the underlying dynamical system. In the stochastic setting this corresponds to the situation where there are disjoint compact subsets $X_j \subset X$, $j = 0, \ldots, r-1$, such that

$$X = \bigcup_{j=0}^{r-1} X_j,$$

and for which the stochastic transition function p satisfies

$$p(x, X_{j+1 \bmod r}) = \begin{cases} 1 & \text{if } x \in X_j \\ 0 & \text{otherwise.} \end{cases} \tag{4.4}$$

We now relate the cyclic dynamical behavior described by (4.4) to spectral properties of the corresponding Perron-Frobenius operator P.

PROPOSITION 4.9 *If the stochastic transition function p satisfies (4.4) then the following statements hold:*

(a) The r-th power P^r of the Perron-Frobenius operator P has an eigenvalue one of multiplicity at least r. Moreover, there are r corresponding invariant measures $\mu_k \in \mathcal{M}$, $k = 0, 1, \ldots, r-1$, with support on X_k, that is, $\operatorname{supp}(\mu_k) \subset X_k$. *These measures can be chosen to satisfy*

$$\mu_k = P^k \mu_0, \quad k = 0, 1, \ldots, r-1.$$

(b) The r-th roots of unity ω_r^k, $k = 0, 1, \ldots, r-1$, where $\omega_r = e^{2\pi i/r}$, are eigenvalues of P.

A proof of this result can be found in Dellnitz and Junge (1999).

The Galerkin Method

We begin with the following observation which immediately follows from standard results on integral operators (see e.g. Yosida (1980), p. 277).

LEMMA 4.10 *Suppose that the transition density function k satisfies*

$$\iint |k(x,y)|^2 \, dm(x) dm(y) < \infty. \tag{4.5}$$

Then the Perron-Frobenius operator $P : L^2 \to L^2$ is compact.

From now on we consider the case where P is given by a dynamical process with a transition density function k satisfying the condition (4.5). The aim is to use a Galerkin method for the approximation of such a Perron-Frobenius operator together with its spectrum. More precisely, let V_d, $d \geq 1$, be a sequence of d–dimensional subspaces of L^2 and let $Q_d : L^2 \to V_d$ be a projection such that Q_d converges point wise to the identity on L^2. If we define the approximating operators by $P_d = Q_d P$ then we have

$$\|P_d - P\|_2 \to 0 \quad \text{as } d \to \infty.$$

Since P is compact one can use standard results from operator theory in order to approximate the eigenvalues of P which are lying on the unit circle by a Galerkin method. For this we construct a Galerkin projection which preserves cyclic behavior in the approximation. Suppose that (4.4) holds and let $\{\varphi_i^j\}$, $j = 0, 1, \ldots, r-1$, $i = 1, 2, \ldots, d_j$, be a basis of V_d with the following properties:

$$\begin{aligned} &\text{(i)} \quad \operatorname{supp}(\varphi_i^j) \subset X_j \quad (j = 0, 1, \ldots, r-1, \quad i = 1, 2, \ldots, d_j), \\ &\text{(ii)} \quad \sum_{i=1}^{d_j} \varphi_i^j(x) = 1 \quad \text{for all } x \in X_j,\ j = 0, 1, \ldots, r-1. \end{aligned} \tag{4.6}$$

REMARK 4.11 In Section 8 we will show how to generate a basis satisfying (4.6) in practice. In that case, V_d will consist of functions which are locally constant.

The Galerkin projection $Q_d g$ of $g \in L^2$ is defined by

$$(Q_d g, \varphi_i^j) = (g, \varphi_i^j) \quad \text{for all } i, j,$$

where $(\cdot, \cdot)$ is the usual inner product in L^2. The following result is a generalization of Lemma 8 in Ding et al. (1993), where just the fixed point of P is considered. Its proof can be found in Dellnitz and Junge (1999). Recall that $\omega_r = e^{2\pi i/r}$.

PROPOSITION 4.12 *Suppose that the Galerkin projection satisfies (4.6). Then the approximating operators $P_d = Q_d P$ also possess the eigenvalues ω_r^k, $k = 0, 1, \ldots, r-1$.*

A combination of standard results on the approximation of spectra of compact operators (see e.g. Osborn (1975)) with Proposition 4.12 yields a convergence result for eigenvectors corresponding to eigenvalues of P of modulus one.

COROLLARY 4.13 *Suppose that P and its approximation P_d satisfy the hypotheses stated above. Then each simple eigenvalue $e^{2\pi ik/r}$ of P on the unit circle is an eigenvalue of P_d and there are corresponding eigenvectors g_d of P_d converging to an eigenfunction h of P. More precisely, there is a constant $C > 0$ such that for all $d \geq 1$*

$$\|h - g_d\|_2 \leq C\|P_d - P\|_2.$$

4.3 Convergence Result for SRB-Measures

Suppose that the diffeomorphism f possesses a hyperbolic attractor Λ with an SRB-measure μ_{SRB}, and let p_ε be a small random perturbation of f. Then, under certain hypotheses on p_ε, it is shown in Kifer (1986) that the invariant measures of p_ε converge in a weak*–sense to μ_{SRB} as $\varepsilon \to 0$. On the other hand one can approximate the relevant eigenmeasures of P_ε by Corollary 4.13 and this leads to the desired result.

THEOREM 4.14 *Suppose that the diffeomorphism f has a hyperbolic attractor Λ, and that there exists an open set $U_\Lambda \supset \Lambda$ such that*

$$k_\varepsilon(x, y) = 0 \quad \text{if } x \in \overline{f(U_\Lambda)} \text{ and } y \notin U_\Lambda.$$

Then the transition function p_ε in (4.3) has a unique invariant measure π_ε with support on Λ and the approximating measures

$$\mu_d^\varepsilon(A) = \int_A g_d^\varepsilon \, dm$$

converge in a weak–sense to the SRB–measure μ_{SRB} of f as $\varepsilon \to 0$ and $d \to \infty$,*

$$\lim_{\varepsilon \to 0} \lim_{d \to \infty} \mu_d^\varepsilon = \mu_{SRB}. \tag{4.7}$$

4.4 Numerical Examples

We present two examples for the set oriented numerical computation of invariant measures. Although the convergence result Theorem 4.14 is stated in the randomly perturbed context these numerical computations are performed using the unperturbed dynamical systems.

EXAMPLE 4.15 Let us begin with a one-dimensional example, the Logistic Map $f : [0,1] \to [0,1]$,

$$f(x) = \lambda x(1-x)$$

for $\lambda = 4$. The unique absolutely continuous invariant measure μ of f has the density

$$h(x) = \frac{1}{\pi\sqrt{x(1-x)}}$$

(see e.g. Lasota and Mackey (1994)). Discretizing the Perron-Frobenius operator on the space of simple functions on a uniform partition of $[0,1]$ we obtain an approximation of h in terms of a piecewise constant function. Figure 8 shows approximations to h using two different partitions with intervals of size 2^{-4} and 2^{-8} respectively.

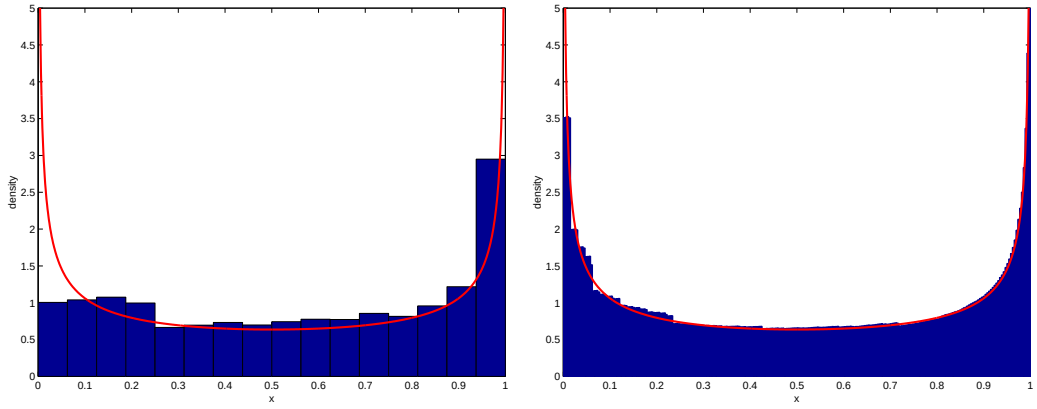

(a) partition with 16 sets

(b) partition with 256 sets

Figure 8: Approximations of the absolutely continuous invariant density of the Logistic Map (black) using piecewise constant functions (gray).

EXAMPLE 4.16 As a more challenging task we consider the approximation of an invariant measure in the Lorenz system (see Section 3.3). We will tackle this by first computing a covering of the underlying invariant set. More concretely the continuation method is used to compute a tight covering of the unstable manifolds of the two nontrivial steady state solutions. Using the space of simple functions on the resulting collection of sets we then compute the stationary vector of the discretized Perron-Frobenius operator as an approximation to an invariant measure.

In Figure 9 we show the result of this computation for the time-0.2-map on subdivision level 30 ($\beta = 1.2$, $Q = [-30, 30] \times [-30, 30] \times [-13, 67]$). A color coding has been used to indicate the values of the invariant density on the covering.

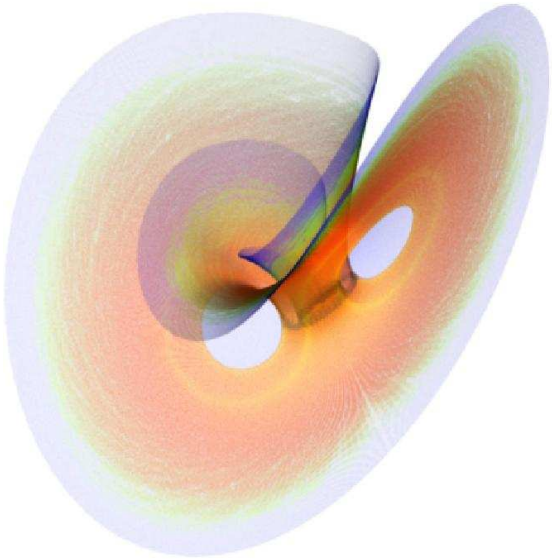

Figure 9: Approximation of an invariant measure in the Lorenz system. The color depicts the density of the (discrete) invariant measure and ranges from blue (lowest density) over pink, green and red to yellow (highest density).

5 The Identification of Cyclic Behavior

Suppose that the stochastic transition function of the randomly perturbed dynamical system satisfies the cycle condition (4.4). Then the purpose is to identify the components X_j.

5.1 Extraction of Cyclic Behavior

By Proposition 4.12 we know that the approximating operator P_d^ε has the eigenvalues ω_r^k, $k = 0, 1, \ldots, r-1$. The cyclic components can be approximated by certain linear combinations of the corresponding eigenvectors.

Two Cyclic Components

In the simplest case, $r = 2$, there are two components X_0 and X_1 which are cyclically permuted by the underlying stochastic process. The idea is to find approximations of eigenmeasures μ_0 and $\mu_1 = P_\varepsilon \mu_0$ of P_ε^2 with support on X_0 and X_1 respectively, see Proposition 4.9. By the same proposition we know that $\omega^0 = 1$ and $\omega^1 = -1$ are eigenvalues of P_ε. Let ν_0 and ν_1 be corresponding (real) eigenmeasures. Then there are $\alpha_0, \alpha_1 \in \mathbb{R}$ such that

$$\nu_0 = \alpha_0(\mu_0 + P_\varepsilon \mu_0) \quad \text{and} \quad \nu_1 = \alpha_1(\mu_0 - P_\varepsilon \mu_0).$$

Rescaling ν_0 and ν_1 so that $\nu_0(X_0) = \nu_1(X_0) = 1$ we can compute μ_0 and μ_1 by

$$\mu_0 = \frac{1}{2}(\nu_0 + \nu_1) \quad \text{and} \quad \mu_1 = \frac{1}{2}(\nu_0 - \nu_1).$$

The same procedure can be applied in order to find appropriate approximations of the probability measures μ_0 and μ_1 for the Galerkin approximation.

General Case

For $\ell = 0, 1, \ldots, r-1$ we denote by $\mu_\ell = P_\varepsilon^\ell \mu_0$ the invariant measure of P_ε^r with support on X_ℓ (see Proposition 4.9).

LEMMA 5.1 *For $s \in \{0, 1, \ldots, r-1\}$ let*

$$\nu_k^s = \sum_{j=0}^{r-1} \omega_r^{-kj} P_\varepsilon^j \mu_s \tag{5.1}$$

be a specific choice for the eigenmeasures of P_ε corresponding to the eigenvalues ω_r^k, $k = 0, 1, \ldots, r-1$. Then

$$\frac{1}{r} \sum_{k=0}^{r-1} \omega_r^{\ell k} \nu_k^s = \mu_{\ell+s \bmod r}.$$

By this lemma we have to find eigenvectors $v_0^s, \ldots, v_{r-1}^s$ of the discretized Perron-Frobenius operator which are approximations of the eigenmeasures ν_k^s in (5.1) for an $s \in \{0, 1, \ldots, r-1\}$. Then we can compute

$$u_{\ell+s \bmod r} = \frac{1}{r} \sum_{k=0}^{r-1} \omega_r^{\ell k} v_k^s$$

for $\ell = 0, 1, \ldots, r-1$, and the positive components of u_j provide the desired information about the support of μ_j on X_j $(j = 0, 1, \ldots, r-1)$.

In the case where the eigenvalues ω_r^k are simple the eigenvectors $v_0^s, \ldots, v_{r-1}^s$ are found as follows. Suppose that we have a set of eigenmeasures ρ_k corresponding to the eigenvalues ω_r^k, $k = 0, 1, \ldots, r-1$. Since the eigenvalues are simple we know that for each $s \in \{0, 1, \ldots, r-1\}$ there is a constant $\alpha_k^s \in \mathbb{C}$ such that ρ_k can be written as

$$\rho_k = \alpha_k^s \nu_k^s.$$

Hence the task is to rescale ρ_k so that $\alpha_k^s = 1$ for all k and this is done by rescaling the ρ_k's by (complex) factors so that for a particular s

$$\rho_k(X_s) = 1 \quad \text{for all } k = 0, 1, \ldots, r-1.$$

With this choice it follows that $\rho_k = \nu_k^s$.

5.2 Numerical Examples

EXAMPLE 5.2 We reconsider Example 2.13 and set $b = 0.2$ and $a = 1.2$. Then the Hénon map possesses a 2-cycle, and we can use the approximation procedure described above to identify the two components X_0 and X_1. In Figure 10 we show the approximations v_0 and v_1 of the two eigenmeasures of the Perron-Frobenius operator corresponding to the eigenvalues $\lambda_0 = 1$ and $\lambda_1 = -1$.

By Lemma 5.1

$$u_0 = \frac{1}{2}(v_0 + v_1) \quad \text{and} \quad u_1 = \frac{1}{2}(v_0 - v_1)$$

are approximations of probability measures μ_0 and μ_1 which have support on X_0 and X_1 respectively. These are shown in Figure 11.

In the computation the box-covering was obtained by the continuation algorithm described in Section 3. The boxes were of size $1/2^{10}$ in each coordinate direction and the continuation was restricted to the square $Q = [-2, 2]^2 \subset \mathbb{R}^2$. This way we have produced a covering of the closure of the one-dimensional unstable manifold of the hyperbolic fixed point in the first quadrant by 2525 boxes.

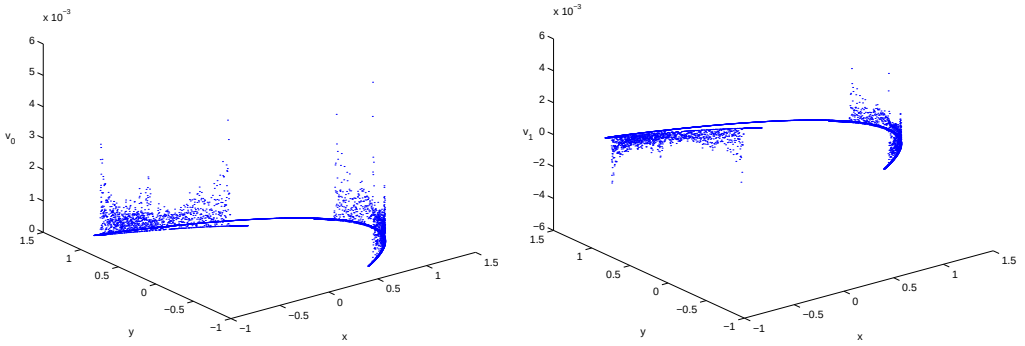

(a) v_0 (b) v_1

Figure 10: Eigenvectors of the approximation of the Perron-Frobenius operator for the Hénon map ($a = 1.2$, $b = 0.2$).

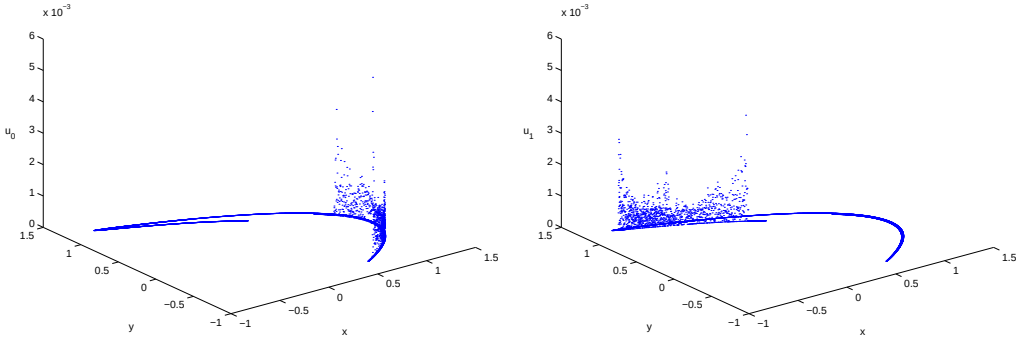

(a) u_0 (b) u_1

Figure 11: Approximations of probability measures with support on the two components of the 2-cycle ($a = 1.2$, $b = 0.2$).

EXAMPLE 5.3 As the second example we slightly modify a mapping taken from Chossat and Golubitsky (1988) and consider the dynamical system $f : \mathbb{C} \to \mathbb{C}$,

$$f(z) = e^{-\frac{2\pi i}{3}} \left((|z|^2 + \alpha)z + \frac{1}{2}\bar{z}^2 \right),$$

for the parameter value $\alpha = -1.7$. For the computation of the box-covering

we have used the subdivision algorithm as described in Section 2. Starting with the square $Q = [-1.5, 1.5]^2$ we have subdivided Q seven times by bisection in each coordinate direction which leads to a box-covering by 3606 boxes. In Figure 12 we show the approximation of the invariant measure, that is, the eigenvector v_0 corresponding to the eigenvalue $\lambda_0 = 1$ of the discretized Perron-Frobenius operator. In this case this operator additionally has the eigenvalues ω_6^k, $k = 1, \ldots, 5$, and hence we may use Lemma 5.1 to compute approximations $v_0, \ldots, v_5$ of the probability measures with support on the cyclic components $X_0, \ldots, X_5$ of a six cycle. These supports are shown in Figure 13.

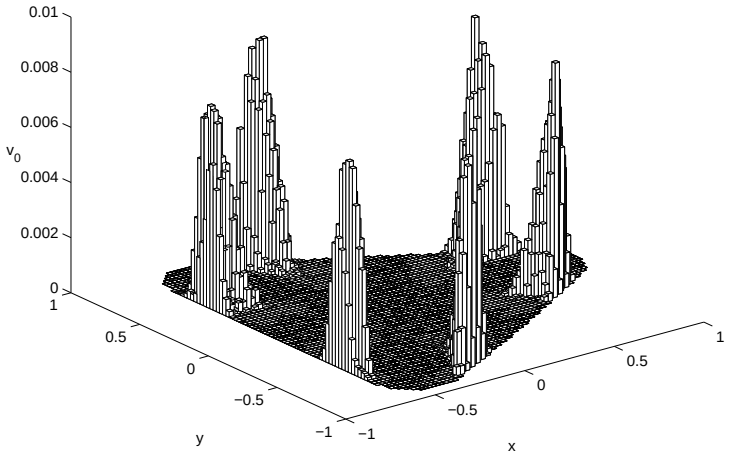

Figure 12: Approximation of the invariant measure for $\alpha = -1.7$.

6 The Computation of Almost Invariant Sets

In the previous sections we have seen that we can approximate the physically relevant invariant measure or even cyclic behavior numerically by an appropriate Galerkin approximation. In practice – in particular in the area of molecular dynamics, Deuflhard et al. (1998); Schütte (1999) – also the approximation of so-called *almost invariant sets* is of relevance. Roughly speaking, these are sets in state space in which typical trajectories stay on

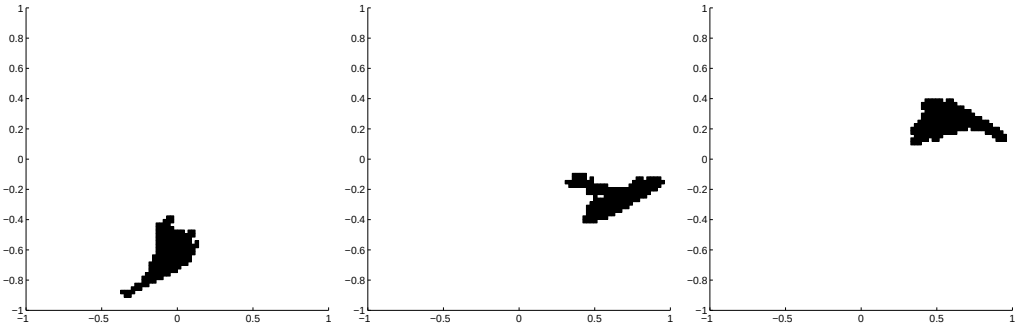

(a) u_0 (b) u_1 (c) u_2

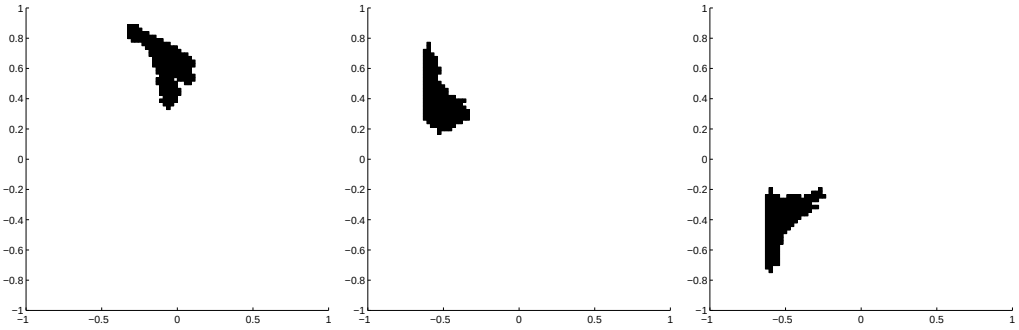

(d) u_3 (e) u_4 (f) u_5

Figure 13: Approximation of the cyclic components $X_0, \ldots, X_5$ for $\alpha = -1.7$.

average for quite a long time before leaving again. The concept of almost invariant sets can naturally be extended to the notion of *almost cyclic behavior*. For simplicity we will restrict to almost invariance but we will illustrate the existence of almost cyclic behavior by a numerical example.

6.1 Almost Invariant Sets

The scenario we have in mind is the following: suppose that a dynamical system possesses two different invariant sets. Correspondingly the Perron-Frobenius operator has a double eigenvalue 1. Then these invariant sets merge while a system parameter is varied. Simultaneously one of the eigenvalues in one moves away from one. The aim is to relate the value of this eigenvalue to the magnitude of *almost invariance* which is still present in the

dynamical system.

EXAMPLE 6.1 (DELLNITZ ET AL. (2000A)) Consider the following parameter dependent family of *FourLegs maps* $T_s : [0,1] \to [0,1]$:

$$T_s x = \begin{cases} 2x, & 0 \le x < 1/4 \\ s(x - 1/4), & 1/4 \le x < 1/2 \\ s(x - 3/4) + 1, & 1/2 \le x < 3/4 \\ 2(x-1) + 1, & 3/4 \le x \le 1 \end{cases}$$

The graph of a typical T is shown in Figure 14. Obviously, for $s = 2$ the

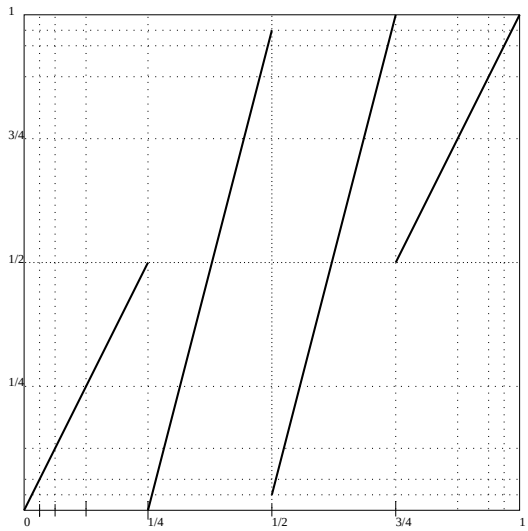

Figure 14: Graph of T_s for $s = 4 - 1/8$.

Perron-Frobenius operator for this map has a double eigenvalue one since both the intervals $[0, 0.5]$ and $[0.5, 1]$ are invariant sets. One can show that the Perron-Frobenius operator has isolated eigenvalues $\lambda_s \neq 1$ for values of s which are arbitrarily close to 2. Moreover these eigenvalues approach 1 while s tends to 2; see Dellnitz et al. (2000a).

As in the case of SRB-measures we work in the following in the context of small random perturbations (see Section 4.1).

DEFINITION 6.2 A subset $A \subset X$ is *δ-almost invariant with respect to $\rho \in \mathcal{M}$* if $\rho(A) \neq 0$ and

$$\int_A p_\varepsilon(x, A)\, d\rho(x) = \delta \rho(A).$$

REMARK 6.3 (a) Using the definition of the stochastic transition function p_ε we compute for a subset $A \subset X$

$$p_\varepsilon(x, A) = \frac{m(A \cap B_{f(x)}(\varepsilon))}{m(B_0(\varepsilon))}.$$

Hence

$$\delta = \frac{1}{\rho(A)} \int_A \frac{m(A \cap B_{f(x)}(\varepsilon))}{m(B_0(\varepsilon))} \, d\rho(x).$$

(b) Recall that $p_\varepsilon(x, \cdot) \to \delta_{f(x)}$ for $\varepsilon \to 0$. Thus, we obtain in the deterministic limit

$$\int_A p_0(x, A) \, d\rho(x) = \int_A \delta_{f(x)}(A) \, d\rho(x) = \rho(f^{-1}(A) \cap A).$$

Therefore in this case δ is the relative ρ-measure of the subset of points in A which are mapped into A.

From now on we assume that $\lambda \neq 1$ is an eigenvalue of P_ε with corresponding real valued eigenmeasure $\nu \in \mathcal{M}_{\mathbb{C}}$, that is,

$$P_\varepsilon \nu = \lambda \nu.$$

In this case $\nu(X) = 0$ (see Remark 4.8 (a)). In the following result, see Dellnitz and Junge (1999), the value of the eigenvalue λ is related to the number δ in Definition 6.2.

PROPOSITION 6.4 *Suppose that ν is scaled so that $|\nu| \in \mathcal{M}$, and let $A \subset X$ be a set with $\nu(A) = \frac{1}{2}$. Then*

$$\delta + \sigma = \lambda + 1, \tag{6.1}$$

if A is δ-almost invariant and $X - A$ is σ-almost invariant with respect to $|\nu|$.

REMARKS 6.5 (a) Observe that in the case where λ is close to one we may assume that the probability measure $|\nu|$ is close to the invariant measure μ of the system.

(b) In the numerical computations we work with the unperturbed equations rather than introducing noise artificially. Thus, it would be important to know whether the eigenvalues of P_0 and P_ε are close to each other for small ε. First results concerning the stochastic stability of the spectrum of the Perron-Frobenius operator are obtained in Blank and Keller (1998).

6.2 Numerical Examples

We illustrate the results by two numerical examples: first we identify numerically two almost invariant sets for Chua's circuit and then we present an almost invariant two cycle for the Hénon map.

EXAMPLE 6.6 Considering the time-0.1-map of Example 2.14 we cover – using the continuation method described in Section 3 – the unstable manifold of the origin by 10372 boxes. In addition to the eigenvalue one the discretized Perron-Frobenius operator does also possess the eigenvalue $\lambda_1 = 0.9272$. We may conclude from this observation that there are two almost invariant sets. Indeed, a coarse numerical approximation of the corresponding regions in phase space leads to the result shown in Figure 15. The result of a more accurate computation is shown in Figure 16. A detailed numerical study of this particular example can be found in Dellnitz and Junge (1997).

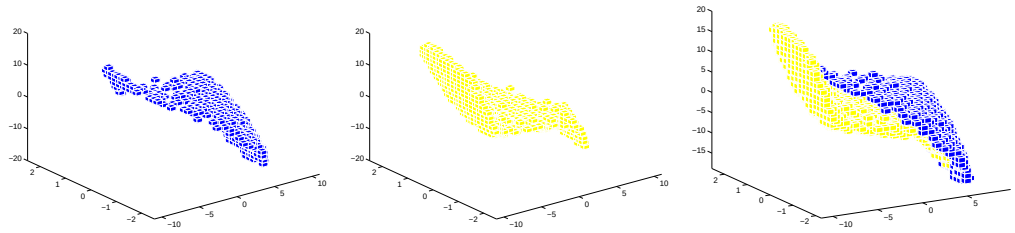

(a) u_1 (b) u_2 (c) u_3

Figure 15: Illustration of the existence of two almost invariant sets in the Chua circuit. (a) Boxes corresponding to components of the approximating densities with value bigger than 10^{-4}; (b) boxes corresponding to components of the approximating densities with value less than -10^{-4}; (c) superposition of the two almost invariant sets.

EXAMPLE 6.7 We reconsider the Hénon map in Example 5.2 and set $a = 1.272$. For this parameter value the two cycle has disappeared, but in simulations the cycling behavior can still be observed for most iterates. Correspondingly we find that $\lambda_1 = -0.9944$ is an eigenvalue of the approximation of the Perron-Frobenius operator. Using the same notation as in Section 5 we show in Figure 17 the approximations of the eigenmeasures. In this case the box-covering consists of 3101 elements.

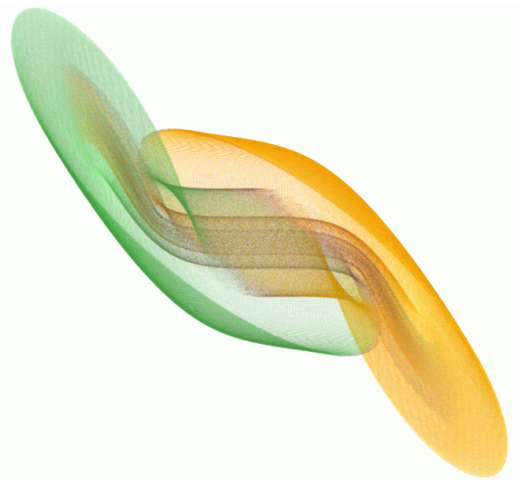

Figure 16: Two almost invariant sets for Chua's circuit.

7 Adaptive Subdivision Strategies

The standard subdivision algorithm may approximate a part of the global attractor which is dynamically irrelevant in the sense that no invariant measure has support on this subset. The reason is that *each* box is subdivided in a step of the subdivision algorithm regardless of any information on the dynamical behavior. In particular, also those subsets of the relative global attractor corresponding to unstable or transient dynamical behavior are approximated by the standard procedure.

On the other hand, if one is mainly interested in the approximation of the support of the (natural) invariant measure rather than in the precise geometric structure of the global attractor then this strategy may lead to unnecessary high storage and computation requirements. In the following we present a modified subdivision strategy (see Dellnitz and Junge (1998)) which avoids this drawback: roughly speaking,

- in the subdivision step we use the information on the actual approximation of the invariant measure to decide whether or not a box should be subdivided;

- in the selection step we keep only those boxes which have a nonempty intersection with the support of the invariant measure.

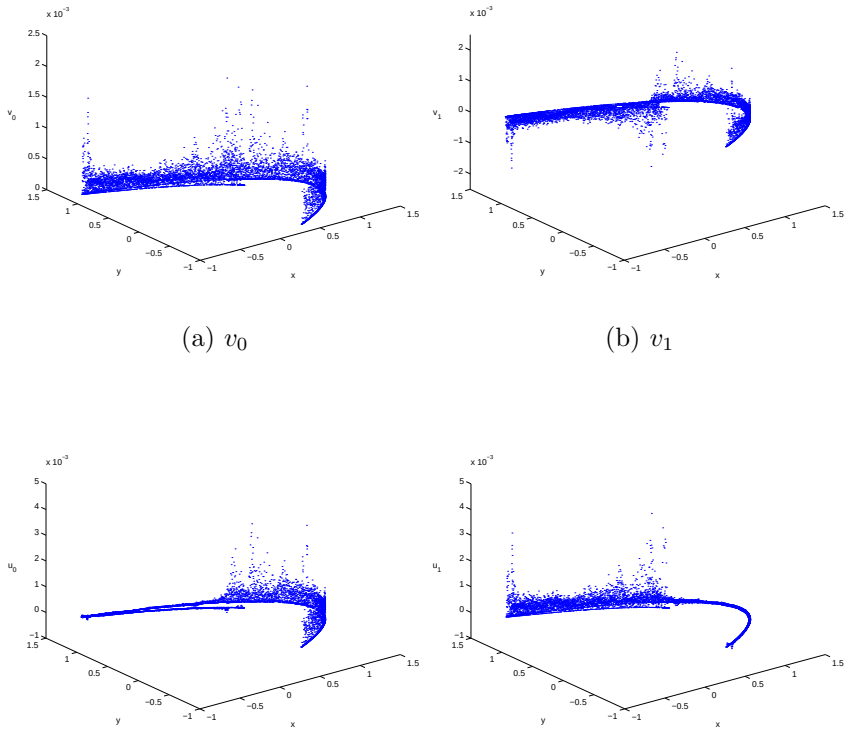

(a) v_0 (b) v_1

(c) u_0 (d) u_1

Figure 17: Eigenvectors v_0, v_1 of the approximation of the Perron-Frobenius operator and approximations u_0, u_1 of probability measures which correspond to the two components of the almost 2-cycle for the Hénon map ($a = 1.272$, $b = 0.2$).

7.1 Adaptive Subdivision Algorithm

Let (δ_k) be a sequence of positive real numbers such that $\delta_k \to 0$ for $k \to \infty$. The algorithm generates a sequence of pairs

$$(\mathcal{B}_0, u_0), (\mathcal{B}_1, u_1), (\mathcal{B}_2, u_2), \ldots$$

where the $\mathcal{B}_k$'s are finite collections of compact subsets of $\mathbb{R}^n$ and the discrete measures $u_k : \mathcal{B}_k \to [0, 1]$ can be interpreted as approximations to an SRB-measure μ_{SRB}:

$$u_k(B) \approx \mu_{SRB}(B) \quad \text{for all } B \in \mathcal{B}_k.$$

Given an initial pair $(\mathcal{B}_0, u_0)$, one inductively obtains $(\mathcal{B}_k, u_k)$ from $(\mathcal{B}_{k-1}, u_{k-1})$ for $k = 1, 2, \ldots$ in three steps:

(i) *Subdivision:* Define

$$\mathcal{B}_{k-1}^+ = \{B \in \mathcal{B}_{k-1} : u_{k-1}(B) \geq \delta_{k-1}\}.$$

Construct a new (sub-)collection $\hat{\mathcal{B}}_k^+$ such that

$$\bigcup_{B \in \hat{\mathcal{B}}_k^+} B = \bigcup_{B \in \mathcal{B}_{k-1}^+} B \quad \text{and} \quad \operatorname{diam}(\hat{\mathcal{B}}_k^+) \leq \theta \operatorname{diam}(\mathcal{B}_{k-1}^+)$$

for some $0 < \theta < 1$.

(ii) *Selection:* Set $\hat{\mathcal{B}}_k = \big(\mathcal{B}_{k-1} \backslash \mathcal{B}_{k-1}^+\big) \cup \hat{\mathcal{B}}_k^+$. Using the space of simple functions on the collection $\hat{\mathcal{B}}_k$ compute a fixed point $\hat{u}_k$ of the discretized Perron-Frobenius operator. Set

$$\mathcal{B}_k = \{B \in \hat{\mathcal{B}}_k : \hat{u}_k(B) > 0\} \quad \text{and} \quad u_k = \hat{u}_k|_{\mathcal{B}_k}.$$

A result on the convergence of this method has been proven in the context of sufficiently regular stochastic transition functions, see Junge (2000) for details.

REMARKS 7.1 (a) In principle there is some freedom in choosing the sequence (δ_k) of positive numbers used in the subdivision step. Note that this sequence determines the number of boxes which will be subdivided and hence it has a significant influence on the storage requirement. In the computations we used

$$\delta_k = \frac{1}{N_k} \sum_{B \in \mathcal{B}_k} u_k(B) = \frac{1}{N_k},$$

where N_k is the number of boxes in $\mathcal{B}_k$.

(b) One can think of more sophisticated ways of choosing the subcollection which is going to be refined in the subdivision step. In fact, one can show that one should aim for an estimate of the *local error* (between the true and the approximate invariant density) and subdivide only those boxes for which this estimate exceeds its average. See Guder and Kreuzer (1999) and Junge (1999) for details on these alternative approaches.

7.2 Numerical Examples

In this section we illustrate the adaptive scheme by two numerical examples. First we consider the Logistic Map again. We will see that, as expected, the adaptive technique is particularly useful if the underlying invariant density has singularities. Additionally we consider the Hénon map as a two-dimensional example and show the box refinement produced by the adaptive subdivision algorithm at a certain step. Again, we refer to Section 8 for details on the numerical realization.

EXAMPLE 7.2 We have approximated the density h of the unique absolutely continuous invariant measure of the Logistic Map using

(a) piecewise constant functions on a uniform partition and

(b) the adaptive subdivision algorithm.

Figure 18 shows the L^1-error between h and the approximate densities versus the cardinality of the partitions.

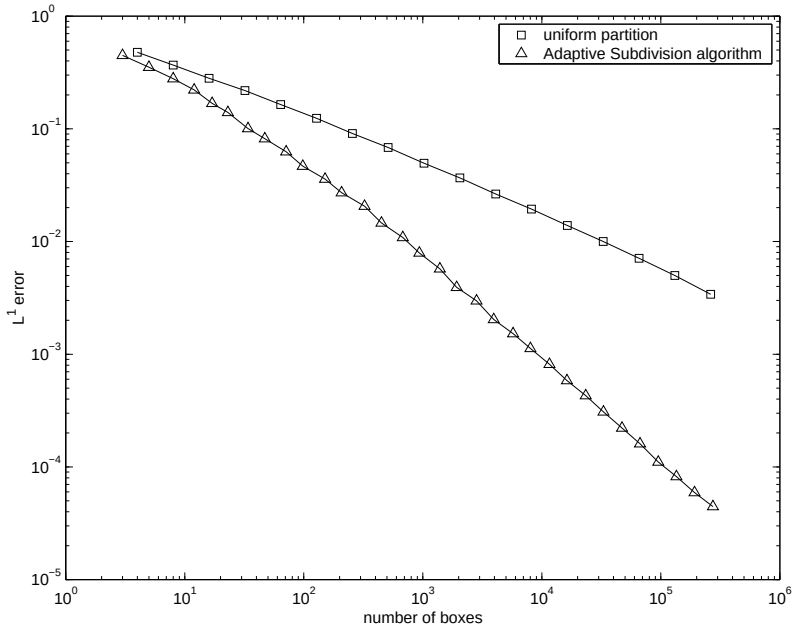

Figure 18: L^1-error between h and the approximate invariant densities versus the cardinality of the underlying partitions

A more detailed analysis of this example using the adaptive algorithm can be found in Murray (1998).

EXAMPLE 7.3 We apply the adaptive subdivision algorithm to the Hénon map, see Example 2.13. In the computations we have chosen the parameters $a = 1.2$, $b = 0.2$, and considered the outer box $\mathcal{B}_0 = \{[-2, 2]^2\}$.

In Figure 19 we present a tiling of the square $[-2, 2]^2$ obtained by the adaptive subdivision algorithm after several subdivision steps. The resulting box-collection $\mathcal{B}$ consists of the grey boxes shown in part (a) of this figure. We expect that due to the numerical approximation some boxes have positive *discrete* measure although they do not intersect the support of the *real* natural invariant measure. Having this in mind we neglect those boxes with very small discrete measure and show in Figure 19(b) a subcollection $\tilde{\mathcal{B}} \subset \mathcal{B}$ with the property that

$$\sum_{B \in \tilde{\mathcal{B}}} u(B) \approx 0.99 \tag{7.1}$$

(see also Remark 7.1(b)). An approximation of a (natural) invariant measure obtained by the adaptive subdivision algorithm is shown in Figure 20.

REMARK 7.4 For the choice of the parameter values we cannot explicitly write down a natural invariant measure. Hence it is impossible to compare the numerical results using analytical ones. Moreover, it is not even known for an arbitrary choice of parameter values whether or not the Hénon map possesses an SRB-measure. However, as already mentioned before, M. Benedicks and L.-S. Young proved that the Hénon map indeed has an SRB-measure for a "large" set of parameter values, see Benedicks and Young (1993).

8 Implementational Details

In this Section we are describing the details of the implementation of the set oriented algorithms. All of the algorithms described in this chapter have been implemented in the software package GAIO which can be obtained from the authors.

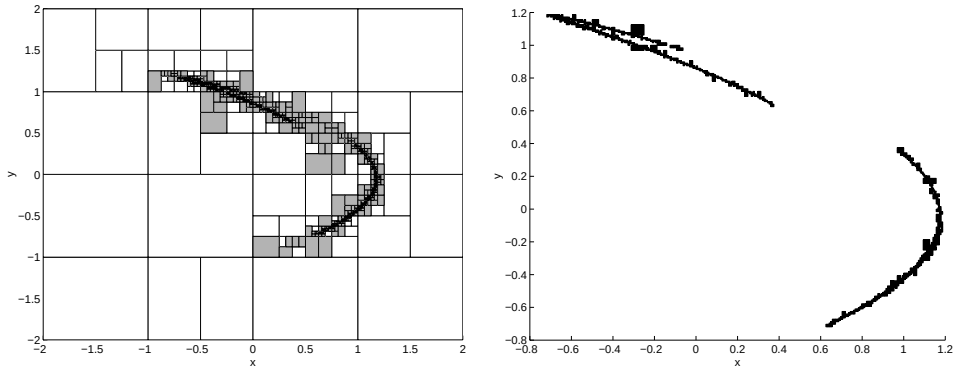

(a) (b)

Figure 19: (a) A tiling of the square $[-2,2]^2$ obtained by the adaptive subdivision algorithm; and (b) the subcollection $\tilde{\mathcal{B}}$ of boxes with discrete density bigger than 0.35 (see also (7.1)).

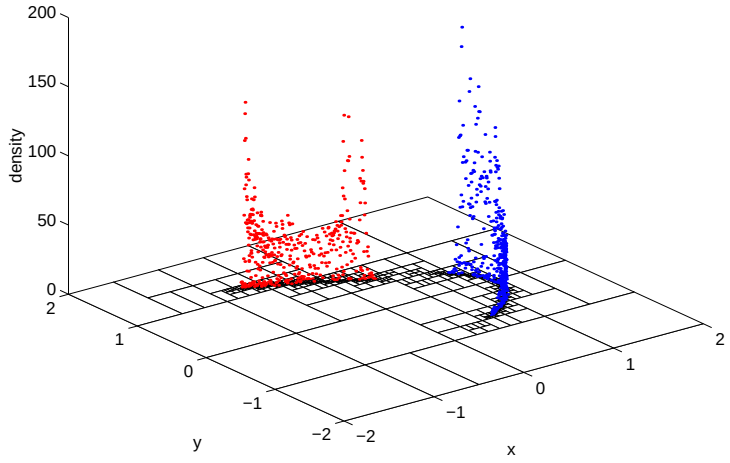

Figure 20: Illustration of a (natural) invariant measure for the Hénon map. The picture shows the density of the discrete measure on $\tilde{\mathcal{B}}$, see (7.1).

8.1 Realization of the Collections and the Subdivision Step

We realize the closed subsets constituting the collections using generalized rectangles ("boxes") of the form

$$B(c,r) = \{y \in \mathbb{R}^n : |y_i - c_i| \leq r_i \text{ for } i = 1,\ldots,n\}\,,$$

where $c, r \in \mathbb{R}^n$, $r_i > 0$ for $i = 1, \ldots, n$, are the center and the radius respectively. In the k-th subdivision step we subdivide each rectangle $B(c, r)$ of the current collection by bisection with respect to the j-th coordinate, where j is varied cyclically, that is, $j = ((k-1) \mod n) + 1$. This division leads to two rectangles $B_-(c^-, \hat{r})$ and $B_+(c^+, \hat{r})$, where

$$\hat{r}_i = \begin{cases} r_i & \text{for } i \neq j \\ r_i/2 & \text{for } i = j \end{cases}, \quad c_i^{\pm} = \begin{cases} c_i & \text{for } i \neq j \\ c_i \pm r_i/2 & \text{for } i = j \end{cases}.$$

Starting with a single initial rectangle we perform the subdivision until a prescribed size σ of the diameter relative to the initial rectangle is reached.

The collections constructed in this way can easily be stored in a binary tree. In Figure 21 we show the representation of three subdivision steps in three dimensions ($n = 3$) together with the corresponding sets Q_k, $k = 0, 1, 2, 3$, see (2.6). Note that each collection and the corresponding covering Q_k are completely determined by the tree structure and the initial rectangle $B(c, r)$.

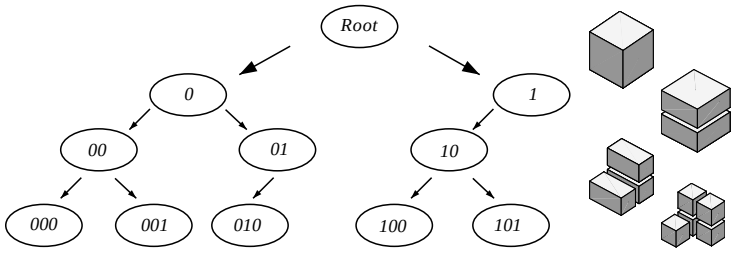

Figure 21: Storage scheme for the collections and the corresponding coverings Q_k, $k = 0, 1, 2, 3$.

8.2 Realization of the Intersection Test

In the subdivision algorithms as well as in the continuation method we have to decide whether for a given collection $\mathcal{B}_k$ the image of a set $B \in \mathcal{B}_k$ has a nonzero intersection with another set $B' \in \mathcal{B}_k$, i.e. whether

$$f(B) \cap B' = \emptyset. \tag{8.1}$$

In simple model problems such as our trivial Example 2.5 this decision can be made analytically. For more complex problems we have to use some kind

of discretization. Motivated by similar approaches in the context of cell-mapping techniques (see Hsu (1992)), we choose a finite set of test points in each set $B \in \mathcal{B}_k$ and replace the condition (8.1) by

$$f(x) \notin B' \text{ for all test points } x \in B\,. \tag{8.2}$$

Obviously, it may still occur that $f(B) \cap B'$ is nonempty although (8.2) is valid.

Distribution of Test Points

It remains to discuss how the test points are distributed inside each rectangle. To define the test points, observe that $R(c,r)$ is the affine image of the standard cube $[-1,1]^n$ scaled by r and translated by c. Using this transformation it is sufficient to define the test points for the standard cube. Simple geometric considerations make it clear that one should obtain the best results for the test in (8.2) if most of the test points are lying on the boundary of the rectangle. An efficient choice for problems of dimension up to three turned out to be N test points on each edge distributed according to

$$t(\ell) = \frac{2\ell - 1}{N} - 1 \quad \text{for } \ell = 1, ..., N \tag{8.3}$$

on $[-1,1]$. As an additional test point we choose the center $c = 0$. Since an n-dimensional rectangle has $n2^{n-1}$ edges, we end up with $p = Nn2^{n-1} + 1$ test points per box.

Rigorous Choice of Test Points

The numerical realization of the intersection test can be made rigorous in the sense that no boxes are lost due to the discretization. Indeed, to accomplish this it is sufficient to have estimates for the Lipschitz constants of the dynamical system f on Q.

To be more precise let $\mathcal{B}$ be a collection of boxes $B = B(c,r) = \{x : |x - c| \le r\}$ (where we write $|x| = (|x_1|, \ldots, |x_n|)$ and $x \le y$ for $x, y \in \mathbb{R}^n$, if $x_i \le y_i$ for $i = 1, \ldots, n$). We need to compute the *set-wise image*

$$\mathcal{F}(B) = \{B' \in \mathcal{B} \mid f(B) \cap B' \neq \emptyset\},$$

for every $B \in \mathcal{B}$. Our goal here is to construct a set $\hat{\mathcal{F}}(B)$ of boxes for which

$$\mathcal{F}(B) \subset \hat{\mathcal{F}}(B),$$

so that we get a rigorous covering of $f(B)$. To this end we will need to know local Lipschitz constants for f, that is, we require that for every box B in the current collection there is a nonnegative matrix $L = L(B) \in \mathbb{R}^{n\times n}$ such that

$$|f(y) - f(x)| \leq L|y - x| \tag{8.4}$$

for $x, y \in B$. If f is continuously differentiable then $L_{ij} = \max_{\xi\in B} |\partial_j f_i(\xi)|$. Now let $h = h(B) \in \mathbb{R}^n$ be a positive vector such that

$$Lh \leq 2r.$$

Using the mesh widths h we now define a mesh

$$\hat{T} = \hat{T}(B) = \{x : (x_i - c_i) \in h_i\mathbb{Z}, i = 1, \ldots, n\}.$$

It is easy to see that for every $y \in B$ there is a meshpoint $x \in \hat{T}(B)$, such that $|y - x| \leq h/2$. On the other hand we are interested in a finite set of test points and indeed the only points $x \in \hat{T}(B)$ we really need are those for which there is actually a $y \in B$ with $|y - x| \leq h/2$. So let

$$T(B) = \hat{T}(B) \cap \{x \mid B \cap \text{int } B(x, h/2) \neq \emptyset\}$$

be the set of test points. Note that an additional constraint on h will be necessary in order to ensure that the test points are contained in B, which is necessary, since the local Lipschitz-estimate (8.4) on f is only valid for points in B. Finally we construct the collection $\hat{\mathcal{F}}(B)$ by setting

$$\hat{\mathcal{F}}(B) = \{\hat{B} \in \mathcal{B} \mid \hat{B} \cap B(f(x), r) \neq \emptyset \text{ for some } x \in T(B)\}. \tag{8.5}$$

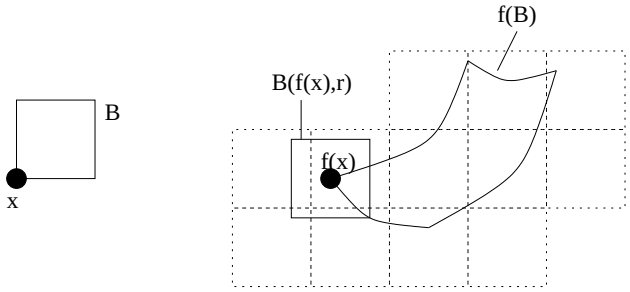

Figure 22: On the construction of $\hat{\mathcal{F}}(B)$.

The idea of this construction is to look at the boxes $B(f(x), r) \notin \mathcal{B}$ corresponding to the images of the test points x and to collect in $\hat{\mathcal{F}}(B)$ all

boxes which have nonempty intersection with those boxes, see Figure 22. It is important to note that the construction of $\hat{\mathcal{F}}(B)$ is a finite task: since the boxes $B(f(x), r)$, $x \in T$, have the same radius as the boxes in the collections $\mathcal{B}$, it suffices to consider the vertices of $B(f(x), r)$.

Adaptive Choice of Test Points

In order to reduce the numerical effort of the set oriented algorithms one has to reduce the number of test points per box as far as possible. We now show how to do that by considering local expansion rates of the map f. To this end we consider the singular value decomposition

$$Df(x) = U(x)S(x)V^{\mathsf{T}}(x)$$

of $Df(x)$, where $U(x) = [u_1(x), \ldots, u_n(x)]$ and $V(x) = [v_1(x), \ldots, v_n(x)]$ are real orthogonal $(n \times n)$-matrices and $S(x) \in \mathbb{R}^{n \times n}$ is a diagonal matrix having the singular values $\sigma_1(x) \geq \cdots \geq \sigma_n(x)$ of $Df(x)$ on the diagonal.

The idea for an improved choice of the test points is to construct a mesh with respect to the basis of right singular vectors $v_1(c), \ldots, v_n(c)$ of $Df(c) = U(c)S(c)V^{\mathsf{T}}(c)$ (where c denotes the center of the box under consideration) and to choose the mesh width h_i, $i = 1, \ldots, n$ in relation to the singular value $\sigma_i(c)$. Let us suppose for the moment that for a box B the derivative $Df(x) = Df(c) = Df = USV^{\mathsf{T}}$ is constant on a sufficiently large neighborhood $\Delta(B)$ of B. Then

$$f(x) - f(y) = Df \cdot (x - y) = USV^{\mathsf{T}}(x - y),$$

so that

$$|f(x) - f(y)| \leq |U|S|V^T(x - y)|$$

where $|U| = (|u_{ij}|)$. We choose mesh widths $h \in \mathbb{R}^n$, $h > 0$, such that

$$|U|Sh \leq 2r \tag{8.6}$$

and define the mesh

$$\hat{T} = \hat{T}(B) = \{x : (V^T(x - c))_i \in h_i\mathbb{Z}, i = 1, \ldots, n\}. \tag{8.7}$$

Again it is easy to see that for every $y \in B$ there is a mesh point $x \in \hat{T}(B)$, such that $|V^T(y - x)| \leq h/2$. We have to restrict ourselves to a finite set of test points again which can be written down as

$$T = T(B) = \hat{T}(B) \cap \{x : B \cap \operatorname{int}(VB(0, h/2) + x) \neq \emptyset\}. \tag{8.8}$$

We construct $\hat{\mathcal{F}}(B)$ as in (8.5) and get that $\mathcal{F}(B) \subset \hat{\mathcal{F}}(B)$. Finally let us consider the general case where $Df(x)$ is not constant on a box. Let

$$M(x) = (m_{ij}(x))_{i,j=1,\ldots,n} = Df(x)V(c)$$

and set

$$\overline{M} = (\overline{m}_{ij})_{i,j=1,\ldots,n}, \quad \overline{m}_{ij} = \max_{x \in \Delta(B)} |m_{ij}(x)|,$$

where $\Delta(B)$ is a sufficiently large neighborhood of B which we suppose to be convex in this case. We choose mesh widths $h > 0$ such that

$$\overline{M}h \leq 2r, \tag{8.9}$$

and use the mesh as defined by (8.7) as well as the construction (8.5) for $\hat{\mathcal{F}}(B)$.

It can easily be shown that the union of boxes in $\hat{\mathcal{F}}(B)$ covers $f(B)$, i.e.

$$\mathcal{F}(B) \subset \hat{\mathcal{F}}(B),$$

see Junge (1999) for details.

8.3 Implementation of the Measure Computation

The feasibility of the computation of invariant measures even for higher dimensional systems relies on the fact that we first compute an outer covering $\mathcal{B}$ of the underlying invariant set by one of the set oriented methods presented in this chapter.

As the ansatz spaces V_d for the discretization of the Perron-Frobenius operator we use the spaces of simple functions on the given collection $\mathcal{B}$. It is easy to see that the discretized Perron-Frobenius operator is then given by a stochastic matrix $P = (p_{ij})$ with entries

$$p_{ij} = \frac{m(f^{-1}(B_i) \cap B_j)}{m(B_j)}, \quad B_i, B_j \in \mathcal{B}.$$

For the computation of the p_{ij}'s we either use a Monte-Carlo approach (see Hunt (1994)) or an exhaustion technique as described in Guder et al. (1997). The latter method is particularly useful when local Lipschitz constants are available for the underlying dynamical system.

For the computation of certain eigenvectors of the resulting (sparse) matrix P an Arnoldi method is used (see Lehoucq et al. (1998)).

Acknowledgments Figures 4, 6, 7, 9 and 16 have been produced using the software platform GRAPE, see Rumpf and Wierse (1992).

References

M. Benedicks and L.-S. Young. Sinai-Bowen-Ruelle measures for certain Henon maps. *Invent. math.*, 112:541–576, 1993.

M. Blank and G. Keller. Random perturbations of chaotic dynamical systems. stability of the spectrum. *Nonlinearity*, 11(5):1351–1364, 1998.

R. Bowen and D. Ruelle. The ergodic theory of axiom a flows. *Invent. math.*, 29: 181–202, 1975.

P. Chossat and M. Golubitsky. Symmetry-increasing bifurcation of chaotic attractors. *Physica D*, 32:423–436, 1988.

C. Conley. *Isolated invariant sets and the Morse index*. American Mathematical Society, 1978.

M. Dellnitz, G. Froyland, and St. Sertl. On the isolated spectrum of the Perron-Frobenius operator. To appear in *Nonlinearity*, 2000a.

M. Dellnitz and A. Hohmann. The computation of unstable manifolds using subdivision and continuation. In H.W. Broer, S.A. van Gils, I. Hoveijn, and F. Takens, editors, *Nonlinear Dynamical Systems and Chaos*, pages 449–459. Birkhäuser, *PNLDE* 19, 1996.

M. Dellnitz and A. Hohmann. A subdivision algorithm for the computation of unstable manifolds and global attractors. *Num. Math.*, 75:293–317, 1997.

M. Dellnitz and O. Junge. Almost invariant sets in Chua's circuit. *Int. J. Bif. and Chaos*, 7(11):2475–2485, 1997.

M. Dellnitz and O. Junge. An adaptive subdivision technique for the approximation of attractors and invariant measures. *Comput. Visual. Sci.*, 1:63–68, 1998.

M. Dellnitz and O. Junge. On the approximation of complicated dynamical behavior. *SIAM J. Numer. Anal.*, 36(2):491–515, 1999.

M. Dellnitz, O. Junge, M. Rumpf, and R. Strzodka. The computation of an unstable invariant set inside a cylinder containing a knotted flow. In *Proceedings of Equadiff '99, Berlin*, 2000b.

M. Dellnitz, O. Schütze, and St. Sertl. Finding zeros by multilevel subdivision techniques. Submitted to *IMA Journal of Numerical Analysis*, 2000c.

P. Deuflhard, M. Dellnitz, O. Junge, and Ch. Schütte. Computation of essential molecular dynamics by subdivision techniques I: basic concept. In P. Deuflhard, J. Hermans, B. Leimkuhler, A.E. Mark, S. Reich, and R.D. Skeel, editors, *Computational Molecular Dynamics: Challenges, Methods, Ideas.*, volume 4 of *Lecture Notes in Computational Science and Engineering*, pages 98–115. Springer, 1998.

P. Deuflhard, W. Huisinga, A. Fischer, and Ch. Schütte. Identification of almost invariant aggregates in reversible nearly uncoupled Markov chains. *Linear Algebra and its Applications*, 315:39–59, 2000.

J. Ding, Q. Du, and T. Y. Li. High order approximation of the Frobenius-Perron operator. *Appl. Math. Comp.*, 53:151–171, 1993.

J. Ding and A. Zhou. Finite approximations of Frobenius-Perron operators. A solution of Ulam's conjecture to multi-dimensional transformations. *Physica D*, 1-2:61–68, 1996.

J. R. Dormand and P. J. Prince. Higher order embedded runge-kutta formulae. *J. Comp. Appl. Math.*, 7:67–75, 1981.

M. Eidenschink. *Exploring Global Dynamics: A Numerical Algorithm Based on the Conley Index Theory*. PhD Thesis, Georgia Institute of Technology, 1995.

G. Froyland. *Estimating Physical Invariant Measures and Space Averages of Dynamical Systems Indicators*. PhD thesis, University of Western Australia, 1996.

G. Keller. Stochastic stability in some chaotic dynamical systems. *Monatsh. Math.*, 94:313–333, 1982.

J. Guckenheimer and Ph. Holmes. *Nonlinear Oscillations, Dynamical Systems, and Bifurcations of Vector Fields*. Springer, 1983.

R. Guder, M. Dellnitz, and E. Kreuzer. An adaptive method for the approximation of the generalized cell mapping. *Chaos, Solitons and Fractals*, 8(4):525–534, 1997.

R. Guder and E. Kreuzer. Control of an adaptive refinement technique of generalized cell mapping by system dynamics. *J. Nonl. Dyn.*, 20(1):21–32, 1999.

H. Hsu. Global analysis by cell mapping. *Int. J. Bif. Chaos*, 2:727–771, 1992.

Fern Y. Hunt. A Monte Carlo approach to the approximation of invariant measures. *Random & Computational Dynamics*, 2(1):111–133, 1994.

O. Junge. *Mengenorientierte Methoden zur numerischen Analyse dynamischer Systeme*. PhD thesis, University of Paderborn, 1999.

O. Junge. An adaptive subdivision technique for the approximation of attractors and invariant measures. Part II: Proof of convergence. Submitted, 2000.

H. Keller and G. Ochs. Numerical approximation of random attractors. In *Stochastic dynamics*, pages 93–115. Springer, 1999.

Yu. Kifer. General random perturbations of hyperbolic and expanding transformations. *J. Analyse Math.*, 47:111–150, 1986.

E. Kreuzer. *Numerische Untersuchung nichtlinearer dynamischer Systeme*. Springer, 1987.

A. Lasota and M.C. Mackey. *Chaos, Fractals and Noise*. Springer, 1994.

A. Lasota and J.A. Yorke. On the existence of invariant measures for piecewise monotonic transformations. *Transactions of the AMS*, 186:481–488, 1973.

R. B. Lehoucq, D. C. Sorensen, and C. Yang. *ARPACK users' guide*. Society for Industrial and Applied Mathematics (SIAM), Philadelphia, PA, 1998. ISBN 0-89871-407-9. Solution of large-scale eigenvalue problems with implicitly restarted Arnoldi methods.

T.-Y. Li. Finite approximation for the Frobenius-Perron operator. A solution to Ulam's conjecture. *J. Approx. Theory*, 17:177–186, 1976.

K. Mehlhorn. *Data Structures and Algorithms*. Springer, 1984.

R. Murray. Adaptive approximation of invariant measures. Preprint, 1998.

J.E. Osborn. Spectral approximation for compact operators. *Math. Comp.*, 29 (131):712–725, 1975.

G. Osipenko. Construction of attractors and filtrations. In K. Mischaikow, M. Mrozek, and P. Zgliczynski, editors, *Conley Index Theory*, pages 173–191. Banach Center Publications 47, 1999.

D. Ruelle. A measure associated with axiom a attractors. *Amer. J. Math.*, 98: 619–654, 1976.

M. Rumpf and A. Wierse. GRAPE, eine objektorientierte Visualisierungs– und Numerikplattform. *Informatik, Forschung und Entwicklung*, 7:145–151, 1992.

Ch. Schütte. *Conformational Dynamics: Modelling, Theory, Algorithm, and Application to Biomolecules*. Habilitation thesis, Freie Universität Berlin, 1999.

M. Shub. *Global stability of dynamical systems*. Springer, 1987.

Y.G. Sinai. Gibbs measures in ergodic theory. *Russ. Math. Surv.*, 166:21–69, 1972.

W. Tucker. The Lorenz attractor exists. *C. R. Acad. Sci. Paris Sér. I Math.*, 328 (12):1197–1202, 1999. ISSN 0764-4442.

S. M. Ulam. *A collection of mathematical problems.* Interscience, 1960.

K. Yosida. *Functional Analysis*. Springer, 1980.